DESIGN AND ANALYSIS OF MULTIBAND CIRCULARLY POLARIZED AND RECONFIGURABLE DIELECTRIC RESONATOR ANTENNAS

Thesis
Submitted in partial fulfillment of the requirements for the degree of

DOCTOR OF PHILOSOPHY

by

USHA L

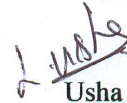**DEPARTMENT OF ELECTRONICS & COMMUNICATION ENGINEERING**

NATIONAL INSTITUTE OF TECHNOLOGY KARNATAKA
SURATHKAL, MANGALORE - 575025, INDIA

DECEMBER 2022

DECLARATION

I hereby declare that the Research Thesis entitled **DESIGN AND ANALYSIS OF MULTIBAND CIRCULARLY POLARIZED AND RECONFIGURABLE DIELECTRIC RESONATOR ANTENNA** which is being submitted to the **National Institute of Technology Karnataka, Surathkal** in partial fulfillment of the requirements for the award of the Degree of **Doctor of Philosophy** in **Electronics and Communication Engineering** is a *bonafide report of the research work carried out by me*. The material contained in this thesis has not been submitted to any University or Institution for the award of any degree.

Usha L
Register No.: 187EC013
Department of Electronics and Communication Engineering
Place: NITK Surathkal

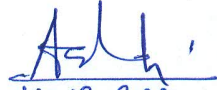Place: NITK, Surathkal.

Date: December, 2022

CERTIFICATE

This is to *certify* that the Research Thesis entitled **DESIGN AND ANALYSIS OF MULTIBAND CIRCULARLY POLARIZED AND RECONFIGURABLE DIELECTRIC RESONATOR ANTENNA** submitted by **USHA L**, (Register Number: 187088EC013) as the record of the research work carried out by her, is *accepted as the Research Thesis submission* in partial fulfilment of the requirements for the award of degree of **Doctor of Philosophy**.

Dr. Krishnamoorthy K.
(Research Guide)
Assistant Professor
Department Electronics and Communication Engg.
NITK Surathkal - 575025

19-12-2022

Prof. Ashvini Chaturvedi
Chairman - DRPC
(Signature with Date and Seal)

ACKNOWLEDGEMENTS

ABSTRACT

The development of wireless communication has led to the improvement in antenna technology. The design and development of dielectric resonator antenna have become challenging to meet the demands of modern wireless communication due to a shift in the increased frequency spectrum. These antennas play a significant role in wireless communication devices in terms of performance parameters and radiation characteristics. Hence, this thesis presents novel dielectric resonator antenna (DRA) designs that provide different radiating bands and patterns for applications related to satellite communication and other wireless devices.

In order to meet the required characteristics, canonical shaped dielectric resonators have been used, which involves less fabrication complexity with aperture feeding. The thesis presents aperture coupled dielectric resonator antennas designed to operate at triband, circular polarization and offers reconfigurability between two bands.

The different slots are used with a rectangular and cylindrical dielectric resonator that operates with triband, circular polarization and frequency reconfiguration. A triangular slot with a cylindrical dielectric resonator antenna is used to obtain triband with hybrid radiating modes with pattern diversity. A hybrid reconfigurable antenna is designed using a triangular slot and a PIN diode in the feed line to obtain dual mode frequency reconfiguration. A flag-shaped feed with a triangular slot helps to achieve a triband circular polarized cylindrical dielectric resonator antenna using the concept of degenerative modes.

Another design presented in this thesis involves an elliptical slot that offers circular polarization in a rectangular dielectric resonator antenna. The slot overlaps two orthogonal modes to produce circular polarization. In another design, a pair of metallic strips acting as a load to a rectangular dielectric resonator is used to obtain circular polariza-

tion for a fixed antenna geometric.

The sense of polarization is varied by changing the orientation of flag-shaped feed in cylindrical DRA, elliptical slot and metallic strips in rectangular DRA. All the designs are fabricated and different antenna parameters are compared based on simulated and fabricated results. The simple DRAs are designed and the performance measures are compared with earlier works presented in terms of impedance bandwidth, gain, axial ratio bandwidth, axial ratio beam width, DRA volume and radiation efficiency.

TABLE OF CONTENTS

LIST OF FIGURES

LIST OF TABLES

ABBREVIATIONS

AR	Axial ratio
ARBW	Axial ratio bandwidth
CP	Circular Polarization
CDRA	Cylindrical Dielectric Resonator Antenna
DRA	Dielectric Resonator Antenna
GPS	
HMSIW	Half Mode Substrate Integrated Waveguide
IoT	Internet of Things
IBW	Impedance bandwidth
LHCP	Left Hand Circular Polarization
LP	Linear Polarization
MMW	Millimeter Wave
MSA	Microstrip Antenna
MMIC	Monolithic Microwave Integrated Circuit
MIMO	Multiple Input Multiple Output
MIC	Microwave Integrated Circuit
RDRA	Rectangular Dielectric Resonator Antenna
RHCP	Right Hand Circular Polarization
RFID	Radio Frequency Identification
SIW	Substrate Integrated Waveguide
WLAN	Wireless Local Area Network
WiMAX	Worldwide Interoperability for Microwave Access
wi-fi	Wireless Fidelity

CHAPTER 1

INTRODUCTION

Today's communication system is becoming wireless due to the advancement of microwave integrated circuit (MIC) technology. An antenna is a crucial element of the wireless communication system. An antenna can be defined as **a transition medium between a guided wave and free space and vice-versa** (Balanis, 2005). It is a kind of transducer that converts electrical energy into electromagnetic and vice versa. A significant additional driving force for the advancement of antenna technology has been the development of wireless communication. A timeline of wireless development is shown in figure 1.1, along with a brief description of applications, Key Performance Indicators (KPIs), network characteristics, and technology, 1G to 6G.

Communication systems require different antennas based on their requirement and advancement in technology. Several research gaps need to be filled in modern wireless communications that require versatile antenna systems. This chapter gives a short introduction to wireless communication and dielectric resonator antennas. The motivation and objectives of the research work are described, followed by the methodology and organization of the thesis.

1.1 Wireless Communication and Dielectric resonator Antennas

Monolithic microwave integrated circuit (MMIC) technology has helped wireless communication grow very fast. Communication has been shifted towards microwave and near millimeter wave frequency side due to overloading existing spectrum and the need for broader bandwidth for wireless applications. As the frequencies to be used increase,
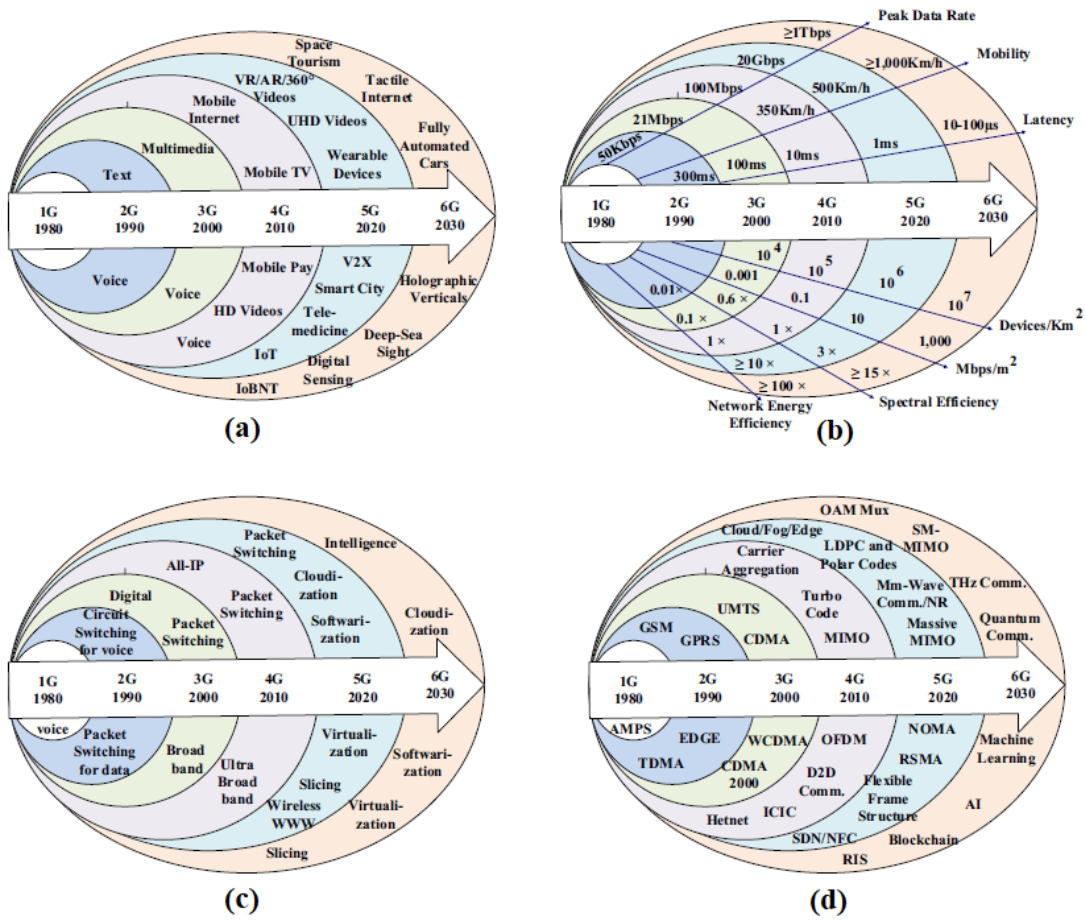
Figure 1.1: Timeline evolution of wireless communication from 1G to 6G based on (a) Applications (b) KPIs (c) Network characteristics and (d) Technological development(Akhtar et al. (2020)).

the dimension of the antennas will decrease and planner. With the advancement of MIC/MMIC technology, antennas are now low profile, compact in design, and integrated with planar systems. To improve the efficiency of wireless communication systems, a number of antennas have been developed, such as wire antennas, aperture antennas, reflector antennas, microstrip patch antennas (MPAs), and dielectric resonator antennas (DRAs). Microstrip patch antennas and dielectric resonator antennas exhibit low profile, ease of fabrication, and ease to excite. The limitation of the microstrip antennas is that these have high conductor and surface wave losses at higher frequencies (Pozar, 2011). DRA's have no conduction losses due to the absence of metal parts; therefore, they can provide better efficiency compared to the microstrip patch antennas.

1.1.1   Mobile Communication

Antennas are a pivotal component of any connected device such as mobile phone or IoT devices. Antennas on today's mobile phones vary from four to thirteen. Mobile phones come with at least four antennas: Wi-Fi, Bluetooth, cellular, and GPS. More antennas are used for FM radio, magnetic Near-Field Communication (NFC) and wireless personal area networks applications. Internet of Things (IoT) devices such as smartwatches, sensors, RFID and many others need a radio link for sending the information. Mobile phones and IoT devices are becoming smaller and increasingly multifunctional. Given the space restrictions in a device, which reduce port-to-port isolation and mutual coupling effects of other elements, it is advantageous to a single antenna structure with several functions. Microstrip monopole based antennas are used. Planar inverted F (PIF) is one of mobile phones' most commonly used antennas. To enable miniaturization, meta-material based patch antennas are used. Microstrip antennas offer a low profile, compact size, and fabrication cost, but they typically suffer from complicated structures, narrow bandwidth, or relatively low gain. The 3D structure of the DRAs makes it possible to design multifunction or diversity DRAs using a single DRA, reducing system size and cost.

1.1.2   Space Communications

With the II world war, radar and military communication technologies gained importance and studies of antennas for space communication started. Early developments in antennas included dish antennas, yagi-uda antennas, horn antennas, array antennas, etc. These antennas are bulky, large, and costly to design, depending on the application. In recent years, antennas used in space communication are expected to have lightweight, low cost, high gain and avoid interference from undesired signals. Microstrip antennas, dipole antennas, microstrip array antennas, dipole array antennas, and other low profile antennas have been developed to meet these demands. In the literature, a number of antenna designs with improved performance are investigated, such as wideband and ultra-wideband, circular and dual-polarization, beam steering, and scanning. In addition

3

to array antennas, Leaky wave antennas are also designed based on the application requirements. Modern technology demands the development of multifunctional antennas that control multiple parameters, including wide bandwidth, polarization control, beam scanning, pattern diversity, radar cross-section (RCS) reduction, sidelobe suppression, low cross-polarization, multiband operation, frequency reconfigurable, high gain and better efficiency. It is possible to achieve the specified requirement with the proper selection of the dielectric resonator in terms of shape, modes and dielectric permittivity. Several high performance multifunction DRAs have been tested and reported in the last decade.

Hence, mobile and space communications have contributed significantly to developing antenna designs with multiple functions appropriate to specific applications. Various communication applications have particular requirements with easy integration of novel antenna systems to meet the demands of fast-growing wireless communication systems.

1.2 Motivation

The current research focuses on dielectric resonator antenna use in microwave and millimeter wave ranges. The dielectric resonator antenna is the best choice over the conventional metallic antennas. Radiation efficiency is very high with these antennas, while metallic antennas lose efficiency with increasing frequency.

The different application uses different frequency band. If a single device is used for a different application, the number of antennas used increases, and the antenna space and cost increase. Multiband antennas are used in applications that operate at different frequency bands simultaneously. A Multiband antenna is a flexible way to communicate with different points at the same time. Multiband antennas are preferred rather than wideband antennas in pre-filtering capability. The receiving antenna front end can reject an undesired frequency spectrum from other systems or spurious emission. With LTE-Advanced's carrier aggregation technique, multiband antennas have become

increasingly important.

Electromagnetic waves are subjected to polarization mismatch and multipath interferences in wireless communication. Circularly polarized (CP) antennas are used to overcome these problems. The CP antennas can reduce Faraday's rotation effect due to the ionosphere in the earth's atmosphere. The CP antennas are used in various wireless systems, including satellite communication, mobile communication, global navigation satellite system (GNSS), wireless sensors, RFID, WLAN, WiMAX and broadcast services. Multiband CP band antennas are developed to have the advantages of both CP antennas and multiband antennas.

Multiband antennas allow mobile wireless devices to coexist on multiple frequency bands with a relatively simple structure and at a relatively low cost. They must use complicated filters with stringent requirements to improve their noise-rejection performance. These filters are generally bulky and expensive. On the other hand, frequency reconfigurable antennas have great potential for reducing production costs and offering better out-of-band noise rejection.

1.3   Problem Definition

Considerable research has been carried out on analyzing DRA shapes. Hemispherical, cylindrical and rectangular DRAs have the exact analytical solution and easy to describe the various field mode configurations, resonant frequency, Q-factor, and radiation patterns. Various multiband, wideband, high gain, linearly polarized, circularly polarized, pattern diversity and polarization diversity DRA are designed.

Multiband antennas are used in multifunctional wireless applications. The major technique in multiband DRAs involves generating higher order modes in the DRA. A higher order mode has a good broadside radiation characteristic and high gain. It is challenging for a given fixed geometric ratio to excite higher order modes in DRA.

CP DRA has been drawing much attention in recent years. CP antennas allow

flexible orientation between the transmitting and receiving antennas popularly used in satellite communication and Global positioning systems(GPS). Various techniques have been used to obtain CP by varying feeding mechanisms modifying the shape of DRA and stacked DRA. In most works, CP is achieved with modification in the DRA shape, which involves fabrication complexity and difficulty in analyzing resonant frequency and radiation characteristics. The analysis of new DRA geometry is difficult. There is a need for a simple feeding mechanism with less/no modification in the shape of DRA, reducing the fabrication design and complexity. There is a requirement for multiband antennas with different polarization and modes. Multiband and CP can be combined in a single antenna to have the advantage of both CP and multiband.

Diversity antennas are more popular in Multiple Input Multiple Output(MIMO) applications to improve performance. Pattern diversity antenna improves performance covering a large area. Different modes generally have different resonance frequencies, leading to a challenge in the diversity antenna design. The reconfigurable antenna can be reconfigured to operate over desired and different frequencies/polarization/patterns. Mechanical movements of the feed line or other radiator parts were used in the early stages of the reconfigurable antenna. A dynamic tuning can be done using electronic, mechanical, physical, or optical switches. The switching biasing circuits and diodes add capacitance and inductance, affecting antenna performance. The complexity of the switching circuit needs to be reduced.

1.4   Objectives

This research work has the following objectives:

- To design a multiband dielectric resonator antenna with higher order hybrid modes using a simple feeding method

- To design a dielectric resonator antenna to provide circular polarization and polarization sense control using different techniques.

- To design a frequency reconfigurable dielectric resonator antenna by using a PIN diode.

The work focus on achieving these objectives in two canonical rectangular and cylindrical dielectric resonator to reduce fabrication complexity.

1.5   Methodology

Several techniques are employed to achieve the proposed objectives. Each antenna design is described below according to the methods used to achieve the desired characteristics. Models are simulated, constructed and measured through the use of lab facilities.

- A triband linearly polarized cylindrical dielectric resonator antenna is designed using a triangular slot aperture feed. Three hybrid modes in C and X bands are excited simultaneously. The triangular slot provides the essential coupling at different points of cylindrical DR to excite the fundamental and higher order modes. A high gain is obtained at higher order mode. In addition, a different radiation pattern is also achieved.

- A circularly polarized rectangular DRA is designed using the elliptical slot. Firstly the rectangular slot is designed to achieve the resonance frequency and is inclined at 45^0 to lower the axial ratio. Further CP bandwidth is achieved by elliptical slot with generation orthogonal resonance frequency. An effort is made to achieve CP in DRA with less fabrication cost.

- A triband circularly polarized cylindrical DRA is designed from a previously designed triband linearly polarized cylindrical DRA. A flag shaped microstrip feed create imperfect PEC and PMC boundary condition. Because of imperfect PEC and PMC boundary conditions, hybrid modes are generated in cylindrical DRA. HE_{m+1n} and EH_{m-1n} modes are generally degenerate. And coupling between the EH and HE modes changes their polarization state and field configuration. Generation orthogonal degenerative modes achieve circular polarization in a higher impedance band.

- In general, CP is generated by overlap orthogonal resonance frequency generated in DRA by the excitation of feed. An effort is made to generate orthogonal resonance frequency by using a metallic strip on the top surface of rectangular DRA. The metallic strip varies the input impedance of DRA and results in other lower resonance frequency.

- To design a dual mode frequency reconfigurable cylindrical DRA using PIN diode. The ON and OFF state of the PIN varies the feed length, which in turn affects the impedance match. Two different modes are excited and have different radiation patterns.

1.6   Organization of the Thesis

The primary aim of this thesis is to design and implement a multiband, multiband CP and frequency reconfigurable DRA using the extensive properties of hybrid modes and canonical dielectric resonators. The thesis is divided into several chapters based on the proposed designs and the results obtained. In the Introduction section of the thesis, we discuss the various requirements and needs of DRA. The motivation is to design a simple, innovative DRA with less fabrication complexity. The objectives, work methodology and thesis organization are provided in this chapter.

The second chapter discusses the concepts of rectangular DRAs, cylindrical DRAs, and their modes. A brief discussion of circular polarization, advantages and disadvantages is also included in this section. The following section includes a brief literature review. It begins with multiband antennas, followed by CP DRAs, multiband CP DRAs, and frequency reconfigurable DRAs. The third chapter discusses a triband cylindrical DRA design to achieve hybrid characteristics. A triangular aperture slot and microstrip feed line are used to excite three hybrid modes with higher order modes in fixed geometric. A cylindrical DRA was designed and experimentally validated in terms of impedance bandwidth and radiation pattern. Three CP DRAs are investigated in the fourth chapter. The first design presents an elliptical slot to achieve two orthogonal modes to obtain a CP wave. The second design achieves CP bandwidth using a triangular slot and flag shaped microstrip feed. And in the third design achieves CP using a metallic strip on the top surface of rectangular DRA. In the fifth chapter, dual mode hybrid reconfigurable cylindrical DRA is designed. A cylindrical dielectric resonator antenna with dual band frequency reconfiguration is proposed. One PIN diode switch is used in the feed line to reconfigure between two bands by turning on and off the switch. A triangular slot is adopted to excite two hybrid modes, which provide a broadside and quasi-end-fire beam pattern. The sixth chapter of the thesis concludes by highlighting the contributions made via different designs. The chapter also highlights the prospects of developing antennas with improved performance for future 5G and biomedical applications.

CHAPTER 2

BACKGROUND AND LITERATURE SURVEY

2.1   Circular polarization

Polarization of electromagnetic waves refers to the direction of the electric field rotation with respect to the wave propagation direction. Polarization is classified as Linear Polarization (LP), Circular Polarization, or Elliptical Polarization (EP) shown in figure 2.1. In LP, the fields oscillate in a single direction. In Circular Polarization and elliptical polarization, the fields rotate at a constant rate in a plane as the wave travels. In CP, the electric field of the light consists of two linear components perpendicular to each other with equal amplitude. In EP, the amplitude of linear components is not the same and/or a phase difference between them is not $\pi/2$.
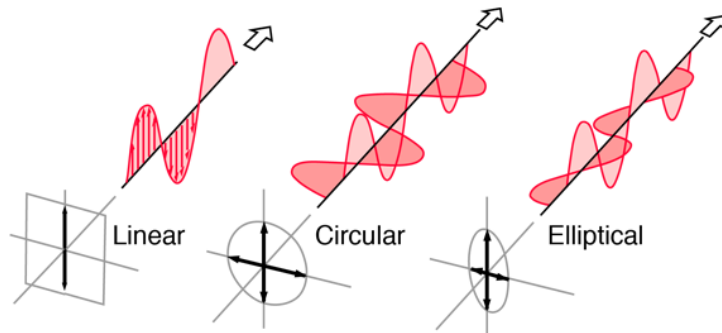
Figure 2.1: Types of polarization (http://hyperphysics.phy-astr.gsu.edu/)

Circular polarization antennas are used to overcome the problems of polarization mismatch and multipath interference. With circular polarization antennas, the plane of polarization rotates in a circular pattern, making one complete rotation during each wavelength. When the rotation is clockwise, the wave is called right-hand circularly polarized (RHCP), while if the rotation is counterclockwise, it is called left-hand circularly polarized (LHCP).

The polarization is measured in terms of Axial Ratio (AR). It is the ratio of the major axis to the minor axis of the curve traced at a given position as a function of time (figure 2.2).
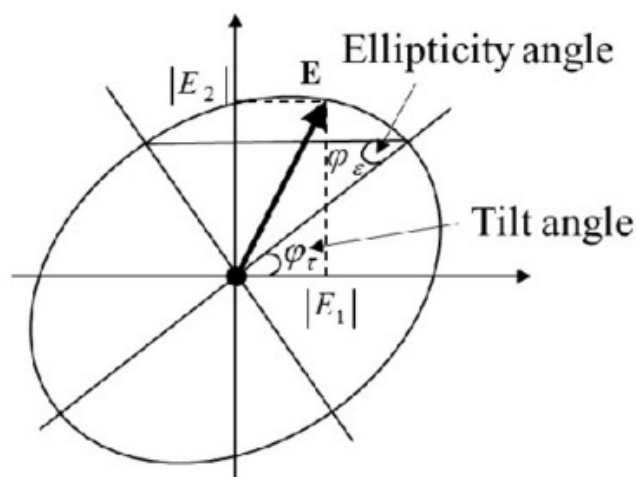
Figure 2.2: The parameters of the polarization ellipse (http://hyperphysics.phy-astr.gsu.edu/).

$$AR = \frac{E_1}{E_2} or \frac{E_2}{E_1} \tag{2.1}$$

Circular Polarization can be achieved only when the magnitude of horizontal and vertical components are the same and the time phase difference between them is $\pi/2$. The instantaneous field of a plane wave traveling in the negative z-direction can be written as

$$\epsilon(z,t) = \vec{a_x}\epsilon_x(z,t) + \vec{a_y}\epsilon_y(z,t) = \vec{a_x}E_{x0}\cos(\omega t + kz + \phi_x) + \vec{a_y}E_{y0}\cos(\omega t + kz + \phi_y) \tag{2.2}$$

For CP $|E_{x0}| = |E_{y0}|$,   AR=1   and $\phi_x - \phi_y = \pm(1/2 + 2n)\pi$ $n = 0, 1, 2, 3..$

Faraday's effect affects linear polarized waves but not a circularly polarized (CP) wave, which is illustrated in figure 2.3. Therefore CP waves are more resistant to signal degradation due to atmospheric conditions. CP waves are much better at penetrating,

10

bending around the obstruction, and overcoming alignment problems.
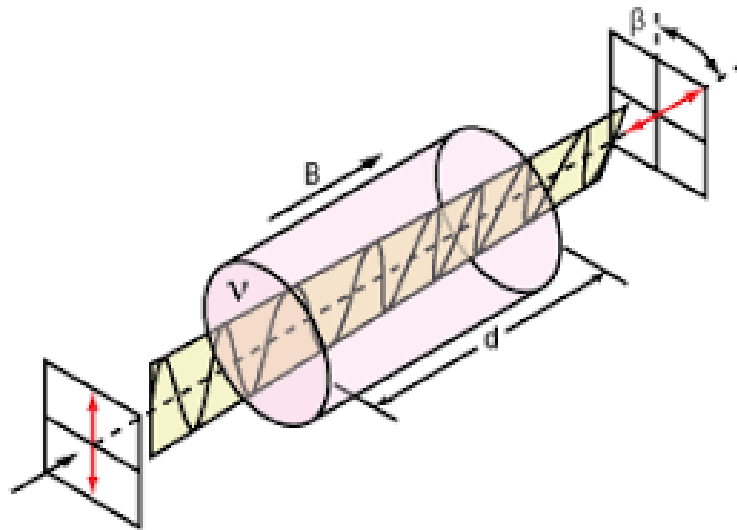
Figure 2.3: Faraday Rotator's Effect on Linearly Polarized Light(http://hyperphysics.phy-astr.gsu.edu/).

2.2   Dielectric Resonator Antenna

The research and development of DRA technology have been a good alternative for the traditional low gain antenna elements. The dielectric resonator was used previously to discover the DRA as a resonator device and a device to store energy. Richtmyer (1939) found that DR could radiate and behave as an antenna. In the 1960s, DR was explored for designing various microwave circuits. Due to its high Q-factor, DR has been widely used for designing filters and oscillators.Long et al. (1983) was the pioneer to demonstrate that DR can be used as an antenna. Good reviews on theoretical and experimental developments of the different DRAs, resonance frequency, feeding techniques, radiation pattern, and their advantages over the traditional antennas are available. (Mongia and Bhartia, 1994; Petosa, 2007; Leung and Luk, 2003; Petosa and Ittipiboon, 2010; Lee et al., 2002; Huitema and Monédière, 2012; Kishk et al., 2006; Guha and Kumar, 2016).

Dielectric Resonator Antennas are non-conducting materials, the mostly ceramic

material used to radiate or receive electromagnetic waves. The dielectric materials are characterized by their dielectric constant. The dielectric material is used in the capacitor to store energy or as resonators in microwave circuits to increase the Q-factor of oscillators and filters. When an electric field is applied, a dipole orientation occurs. Its behavior depends on the situation, which determines how it reacts to the applied field and its induced dipole moment.

Dielectric resonators, when excited, appropriately radiate energy into free space and are known as Dielectric resonator antenna (DRA). Dielectric resonators (DR) can be used as a radiating element was first demonstrated by Long, M C Allister, and Shen in the 1980s. There has been significant progress in DRA technology in the last three decades. The very low metallic loss property of DRA makes it much suitable for high frequency applications. In DRAs, the material of DR is used with a low loss tangent ($\tan\delta = 10^{-4}$ or less). The high permittivity and low value of loss tangent of DR make its quality factor very high (Q$\approx$1/$\tan\delta$ and Q$\approx\epsilon$). The quality factor of the DR remains very high when it is used. Low profile DRA can easily be fabricated by choosing high permittivity DR material. Compact DRAs have been designed for wireless communication and Millimeter-wave application in recent years. DRAs are available in various shapes such as hemispherical, rectangular, cylindrical, etc., as shown in figure 2.4

Figure 2.4: Dielectric Resonator Antenna (Leung and Luk (2003).)

EM waves are introduced into the DRA by a suitable technique that bounces back

and forth between its walls that form standing waves. The walls of the resonator at the interface of dielectric and air are partially transparent to EM waves and radiate into space. The resonance frequency of DRA is determined by its shape, physical dimensions, and dielectric constant. The attractive features of DRAs are:

- The DRA size is proportional to $\frac{\lambda_0}{\sqrt{\epsilon_r}}$. λ_0 and ϵ_r are free space wavelength and relative dielectric permittivity, respectively. ϵ_r allows flexibility in controlling antenna size and bandwidth.

- DRA can be excited by simple feeding methods such as a probe, microstrip, waveguides, slots, substrate integrated waveguide (SIW) and half-mode substrate integrated waveguide (HMSIW).

- The absence of the inherent conductor losses in DRA provides efficient radiation in the millimeter wave(MMW) frequency range compared to microstrip.

- Multiple modes excited in DRA can be employed for different applications.

2.2.1 Radiations Produced in DRA

The dielectric material can be composed of polar or nonpolar molecules. In the case of polar molecules and the absence of an external electrical field, the electric dipoles of molecules are oriented randomly, as shown in figure 2.5a. Suppose the dielectric material is positioned in an external electrical field $\vec{\mathbf{E}}_0$, the polar molecules orient with the external field, as in figure 2.5b. Opposite charges on adjacent dipoles within the volume of dielectric neutralize each other, so there is no net charge within it. The upper and lower surfaces that border the dielectric alignment produce a net charge. Therefore, the external electrical field merely aligns the dipoles, the dielectric as a whole is neutral, and the surface charges induced on its opposite faces are equal and opposite. This induced surface charges $+Q_i$ and $-Q_i$ produce an additional electrical field $\vec{\mathbf{E}}_i$ (an induced electrical field), which opposes the external field $\vec{\mathbf{E}}_0$, as in figure 2.5c.

The same effect is produced when the molecules of a dielectric are nonpolar. In nonpolar molecule acquires an induced electric-dipole moment because the external field $\vec{\mathbf{E}}_0$ causes a separation between its negative and positive charges. The induced dipoles of the nonpolar molecules align with $\vec{\mathbf{E}}_0$ in the same way the permanent dipoles of the polar molecules are aligned as in figure 2.5b.
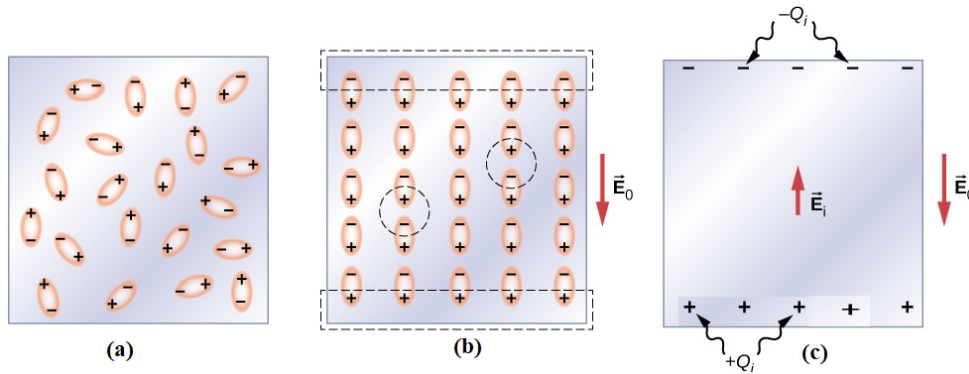
Figure 2.5: Dielectric with polar molecules (https://openpress.usask.ca/).

Therefore, an external electric field brings the charges of the dielectric molecules into a certain ordered arrangement in space and creates an acceleration phenomenon in the dielectric material itself. The dielectric polarization is equal to the total dipole moment induced in the volume of the material by the electric fields. In most cases, the magnitude of polarization is directly proportional to the intensity of the electric field at a given point of a dielectric.

The discontinuity of the relative permittivity at the resonator surface allows a standing electromagnetic wave to be supported in its interior at a particular resonant frequency, thereby leading to maximum energy confinement within the resonator. Thus, there will be a change in the field, contraction, and expansion, which causes the fringing effect. This way dielectric object starts to radiate.

2.2.2 Excitation Techniques

Impedance matching DRA and feed is very important for maximum energy coupling. There are several feeding techniques used for the excitation of modes in DRA. To couple the maximum energy from the excitation source to DRA, a suitable coupling technique is required. Position of excitation with respect to DRA will couple associated electric and magnetic fields corresponding to particular resonating modes. The type and location of the feed method affect the resonant mode, operational frequency, impedance bandwidth and radiation characteristics. Some commonly used excitation techniques

for DRA are summarized below:

Coaxial Probe

Probes can be viewed as vertical electric currents positioned in a way that achieves strong coupling to the DRA. By adjusting the height and diameter of the probe, the level of coupling can be optimized. Different modes can be excited based on the shape of the DRA and location of the probe (Petosa, 2007). Probe feed has the advantages of providing a good coupling even for low permittivity DRAs and it even avoids the need of a matching circuit. In cylindrical DRA, to excite TM_{01} mode, the feed probe is must be located at the center, which gives quarter wavelength monopole radiation patterns and for HEM_{111} mode excitation, the feed probe is located close to the peripheral boundary which results in broadside radiation patterns. In rectangular DRA, a probe located adjacent will excite $TE_{\delta 11}$ mode (Figure 2.6). The coaxial probe feed will also excite undesired modes, especially the higher order modes of the DRA, distorting the primary radiation pattern. Another issue is the probe needs to be protruded into the DRA. Drilling hole to precision in a DRA is a tough challenge

Microstrip Line

The microstrip feed is the simplest method of coupling DRA. Two methods of direct and proximity coupling are used. $TE_{\delta 11}$ is excited rectangular DRA and $HE_{11\delta}$ in cylindrical DRA.

The microstrip line excites magnetic fields in the cylindrical DRA in a short horizontal dipole pattern and short magnetic monopole pattern in rectangular DRA (Figure 2.7) (Petosa, 2007). If the dielectric constant of the material used is low, the amount of energy coupled will be less. However, with an increasing dielectric constant, the antenna size will be reduced at higher frequencies, making the fabrication process very sensitive and producing faulty results. When the magnetic fields in the DRA are excited by a microstrip line, a short horizontal dipole is created, which can be improved by
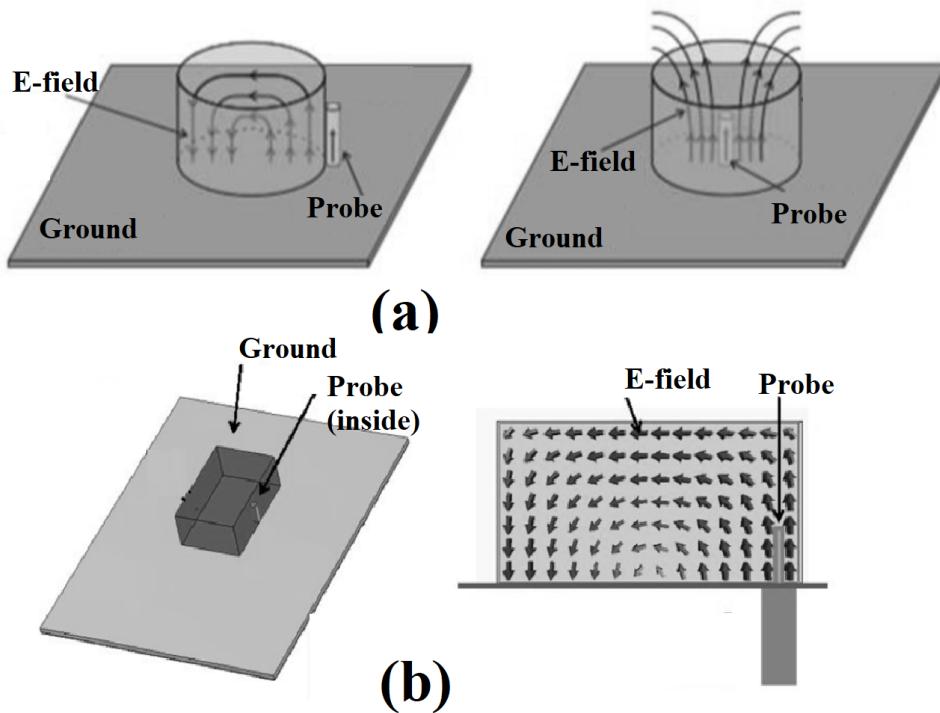
Figure 2.6: Coaxial probe feed excitation (a)$HEM_{11\delta}$ and $TM_{01\delta}$ for CDRA (b) $TE_{11\delta}$ for RDRA

increasing the material's dielectric constant.
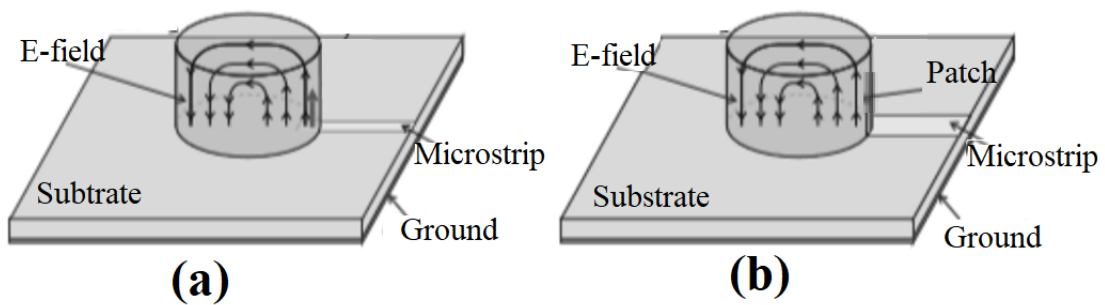
Figure 2.7: Microstrip Line Feed excitation (a)Feed underneath to CDRA (b)Patch feed

Aperture Slot

The DRA is excited through an aperture in the plane of the ground upon which it is positioned. Microstrip lines are used to supply the slot because they can be easily

etched and can be used for impedance matching. The aperture coupling technique has the feed network located below the ground plane. It avoids unwanted radiations that cause distortion and degrade the antenna radiation pattern shape. Different shapes of the slot are used in the literature. In the case of $HEM_{11\delta}$ or TM_{110} dominant resonant mode in cylindrical DRA and $TE_{\delta 11}$ in rectangular DRA (Figure 2.8), the aperture at the DRA center behaves like a magnetic current flowing parallel to it, which excites the magnetic fields in the DRA body and causes broadside radiation patterns (Petosa, 2007).
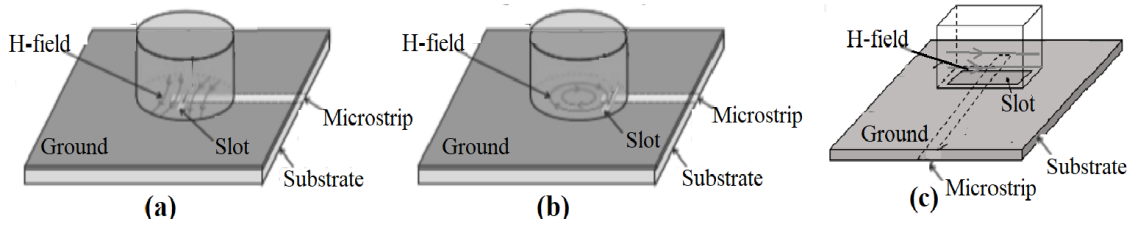
Figure 2.8: Aperture feed excitation (a)$HEM_{11\delta}$ and (b)$TM_{01\delta}$ for CDRA (c)$TE_{11\delta}$ for RDRA

The resonance of the slot is avoided to prevent backward radiation. A slot of small enough dimensions is kept to prevent its resonance from merging with that of the DRA, but a large enough dimension is used to couple a sufficient amount of energy. The printed technology has made the aperture feed with microstrip line an easy approach. Good starting values of slot length and slot width are:

$$l_s = \frac{0.4 \times \lambda_o}{\sqrt{\epsilon}} \tag{2.3}$$

$$w_s = 0.2 \times l_s \tag{2.4}$$

Coplanar Feeds

Coplanar feeds can also be used to couple DRAs. Open-circuit coplanar waveguides can be used to feed DRAs(Figure 2.9a). Adding stubs or loops at the end of the line allows

additional control for impedance matching. Energy is efficiently coupled to the DRA by the coplanar loop. DR elements can be gradually slid over the loop to determine the coupling level and desired mode ($HE_{11\delta}$ or $TE_{01\delta}$) of excitation in cylindrical DRA (Petosa, 2007). Even with coplanar feed, the dimension should be large enough to ensure proper coupling but small enough to avoid excessive radiation in the backlobe.

Substrate Integrated Waveguide

The conventional feeding systems suffer from significant tradeoffs between size, cost and performance at microwave and millimeter wave frequency (Wu et al., 2003). Thus, a new generation of transmission lines for high frequency integrated circuits named substrate integrated waveguides (SIW) has been developed (Figure 2.9b). SIW is made up of metallic vias on a low loss dielectric substrate that acts just like the walls of a waveguide. Because it is constructed from metallic interfaces, it can be fabricated on standard PCBs and integrated seamlessly with DRA. The SIW has high Q-factors and DRA has low loss at millimeter wave frequencies. The SIW-fed DRA is a good candidate for low-loss millimeter wave communication systems. SIW has limited power handling along with dielectric and conductor losses (Venanzoni et al., 2019).
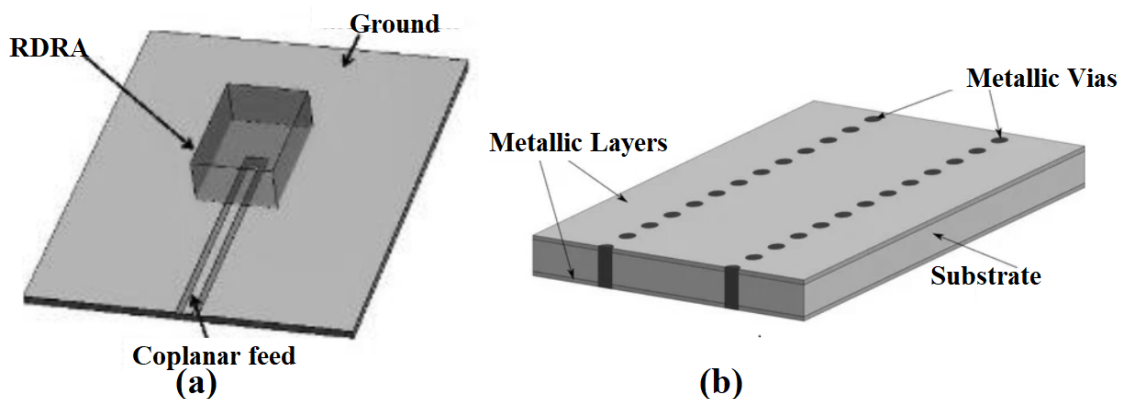
Figure 2.9: (a)Coplanar feed RDRA (b)Physical structure of the substrate-integrated waveguide

18

2.2.3 Cylindrical Dielectric Resonator Antenna

A dielectric resonator antenna in a cylindrical shape is called a cylindrical DRA (CDRA) and offers one degree of freedom in design flexibility. The ratio of radius/height controls the resonant frequency and the Q-factor. Various modes can be easily excited within cylindrical DRA, which results in either broadside or omnidirectional radiation patterns. Transverse magnetic mode (TM), transverse electric mode (TE) and hybrid modes (HEM) are excited in cylindrical DRA. The field pattern of these modes is shown in figure 2.6. TE and TM modes have no dependence on azimuth, while HEM has a dependence on azimuth ϕ. The hybrid modes can be further subdivided into HE and EH modes. For HE modes, the H_z component is quite small compared to the electric component and EH modes the E_z component is quite small compared to the magnetic component The most commonly radiated modes are $TM_{01\delta}, TE_{01\delta}$ and
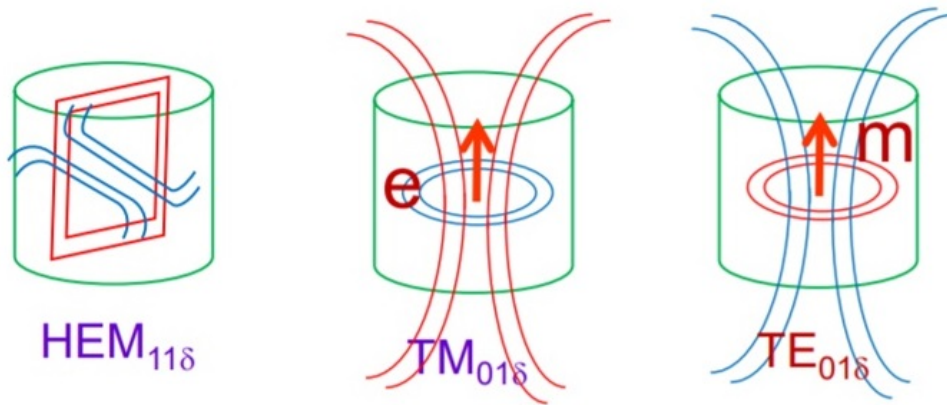
Figure 2.10: Dielectric Resonator Antenna (Leung and Luk (2003)).

$HEM_{11\delta}$. The mode subscript refer to field variations in azimuth, radial and axial direction, respectively. The value of δ ranges between 0 and 1(it approaches 1 for high ϵ_r). Petosa (2007) gives the resonant frequency of a DRA using Modal analysis by assuming perfect magnetic and/or electric walls on the resonator faces is given below. .

$$f_{HEM_{11\delta}} = \frac{6.324c}{2\pi r\sqrt{\epsilon_r + 2}} \left\{ 0.27 + 0.36\frac{r}{2h} + 0.02\left(\frac{r}{2h}\right)^2 \right\} \qquad (2.5)$$

19

$$f_{TE_{01\delta}} = \frac{2.327c}{2\pi\sqrt{\epsilon_r + 1}} \left\{ 1 + 0.2123\frac{r}{h} - 0.000898 \left(\frac{r}{h}\right)^2 \right\} \tag{2.6}$$

$$f_{TM_{01\delta}} = \frac{c\sqrt{3.83^2 + \left(\frac{\pi r}{2h}\right)^2}}{2\pi r\sqrt{\epsilon_r + 2}} \tag{2.7}$$

where h and r are the height and radius of the CDRA. The $HEM_{11\delta}$ modes of the CDRA radiate like a magnetic dipole. A short electric monopole radiation pattern is obtained for $TM_{01\delta}$ while $TE_{01\delta}$ mode resembles a short magnetic monopole. The ideal radiation pattern of $TE_{01\delta}$, $TM_{01\delta}$, $HEM_{11\delta}$, $HEM_{12\delta}$ and $HEM_{21\delta}$ is shown in figure 2.7. The electric field distribution of hybrid modes is shown in figure 2.8.
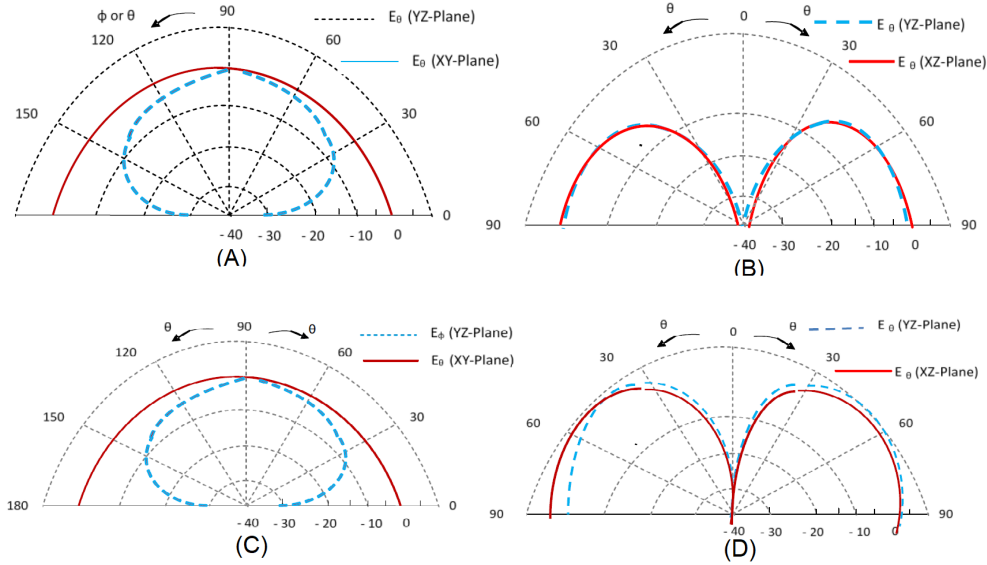
Figure 2.11: Radiation pattern of (A) $TE_{01\delta}$ (B) $TM_{01\delta}$ (C)$HEM_{11\delta}$, $HEM_{12\delta}$ (D)$HEM_{21\delta}$(Leung and Luk (2003)).

$$f_{HEM_{21\delta}} = \frac{1.03c}{2\pi a\sqrt{\epsilon_r + 2}}\sqrt{3.83^2 + \left(\frac{\pi a}{2h}\right)^2} \tag{2.8}$$

20
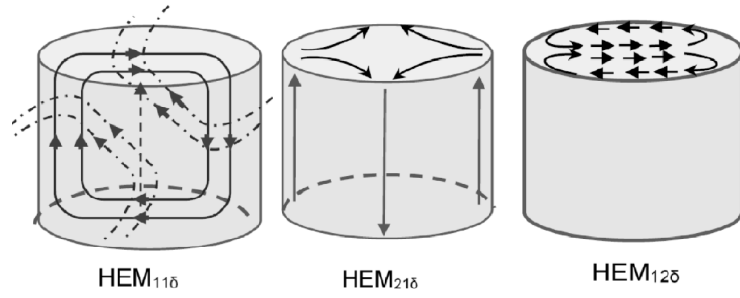
Figure 2.12: Electric field distribution of hybrid modes in CDRA (Kajfez et al. (1984)).

2.2.4 Rectangular Dielectric Resonator Antenna

A dielectric resonator antenna with a rectangular cross section is called a rectangular DRA(RDRA). Rectangular DRA is characterized by three independent lengths, width w, depth d, and height b/2 and has two degrees of freedom in design flexibility, i.e., aspect ratio w/b and d/b.

A dielectric waveguide model is commonly used to analyze rectangular DRA. With this model, the top surface and two sidewalls of DRA are assumed to be perfect magnetic walls, and the other two sidewalls are assumed to be imperfect magnetic walls. TE and TM modes are obtained for RDRAs isolated from a plane. If DRA is mounted on a plane, an electric wall is assumed for the bottom surface. But with rectangular DRA mounted on a plane, only TE modes are excited. TE_{111} mode is the fundamental mode. The TE modes can be along the three directions x, y and z with w>d>b/2, the modes in the order of increasing resonant frequency are $TE_{111}^{x}, TE_{111}^{y}$ and TE_{111}^{z}. The electric field distribution TE_{111} and higher modes are shown in figure 2.9.

The resonant frequency in rectangualr DRA is given below by Petosa (2007).

$$f_{GHz} = \frac{15F}{w_{cm}\pi\sqrt{\epsilon_r}} \tag{2.9}$$

F is the normalized frequency.

$$F = 2.57 - 0.8(d/b) + 0.42(d/b)^2 - 0.05(d/b)^3 + 2.71(d/b)^{(}0.282)(w/b) + 0.16(w/b)^2$$

$$(2.10)$$

The resonant frequency rectangualr DRA is calculated by transcendent equation shown in equation 2.13.

$$k_x^2 + k_y^2 + k_z^2 = \epsilon_r k_0^2 \qquad (2.11)$$

$$k_0 = \frac{2\pi}{\lambda_0} k_y = \frac{\pi}{w} k_z = \frac{\pi}{b} \qquad (2.12)$$

$$k_x \tan(\frac{k_x d}{2}) = \sqrt{((\epsilon_r - 1)k_0^2 - k_x^2)} \qquad (2.13)$$
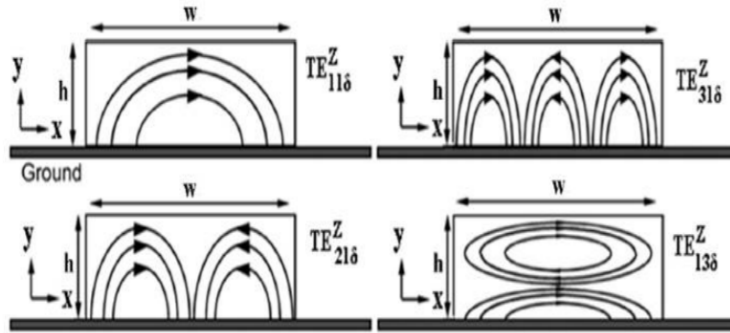
Figure 2.13: TE modes in RDRA (Petosa (2007)).

2.3 Literature Survey

2.3.1 Multiband DRA

In the early development of the DRAs, a narrow bandwidth could be achieved, although broader than a microstrip line antenna. A wideband antenna can cover more frequency bands and improve the efficiency of the communication system. However, subsequent research work has resulted in the enhancement bandwidth of DRA. Early works have been done in widening the impedance bandwidth. Modern Mobile communication in-

cludes various services such as GPS, Wi-Fi, Bluetooth and LTE. Each nation or wireless carrier uses different frequency bands, arise a need for a multiband antenna. The antenna system requires the integration of multiple radiators and operates at multiple bands in civilian and military applications. Research in wireless communication today has significantly focused on multiband antennas because a single radiator can cover several wireless frequency bands and reject the unwanted bands. A wideband antenna covers all frequency points within its operating range. Multiband antennas are essential to provide a multifunctional system. A multiband antenna operates at a particular frequency band but not at intermediate frequencies within these bands. Multiband antennas are preferred rather than the wideband antenna in pre-filtering capability. An undesired frequency spectrum from other systems or spurious emission can be rejected at the receiving antenna front end. With LTE-Advanced's carrier aggregation technique, multiband antennas play a more significant role.

The previous literature reported shows that designing the multiband DRAs is obtained by exciting higher order radiating mode, using parasitic element load DRA, or using the concept of hybrid DRA.

A parasitic C-slot and microstrip line feed is used for the dual band in cylindrical DRA Chen et al. (2008). A frequency band of 2.36-2.5GHz and 5.4-5.8GHZ with a gain of 3dBi and 3.5 dBi, respectively is achieved. A dual band by Ding and Leung (2009) was obtained using zonal slot and DRA. A zonal slot provides the lower band and the upper band is due to DRA modes. The antenna has impedance bandwidth in the lower band is 4.48% and the upper band is 6.17%. Bemani et al. (2011) designed a triple band rectangular DRA that covers various frequency bands such as WLAN 2.4/5.8 and WiMAX 3.5GHz. Three different dimensions of rectangular DRA are used and metal plates are used to separate the DRAs, making the antenna complex structure. Sharma and Brar (2013) used an irregular pentagon shape DRA for triple band 2.42-2.61GHz,3.15-4.05GHz,5-5.65GHz with percentage matching bandwidth of 7.55%, 23.77% and 12.2% respectively. The fabrication of an irregular pentagon shaped with an accurate angle and the side length is difficult. Multiband is generated by exciting higher order radiating modes in the DRA (Guha et al., 2011, 2014). $HEM_{12\delta}$

23

and $HEM_{21\delta}$ were excited with fundamental modes $HEM_{11\delta}$ and HEM_{111} in CDRA. Excitation of higher order modes is challenging for a fixed antenna geometric. Multi-band CDRA with five radiating modes is proposed in Sharma et al. (2017a) suitable for WLAN and WiMAX applications. Five different radiating modes are obtained with diversified radiation patterns. A vertical strip along with a modified microstrip feed is used. In Khan et al. (2016) stacked modified RDRA is used to obtain multiband for LTE applications. Lin et al. (2019) a triband MIMO RDRA is designed for LTE application. The hybrid technique is adopted by combining a meander line antenna with an RDRA to have a multiband. The three frequencies are 0.9GHz, 1.8GHz and 2.3GHz with approximately 5%, 11% and 3% bandwidth.

The use of parasitic elements and hybrid DRA to achieve multiband is complex. It is advantageous to obtain multiband by exciting higher order modes in the DRA, to have advantages of DRA. Aperture coupling feed is efficient and easy compared to coaxial feed and microstrip feed in DRA.

2.3.2   Circularly Polarized DRAs

The circularly polarized antenna has the advantage of mitigating multipath fading and immunity to polarization mismatching and is widely used in wireless and satellite communication. The DRA can generate CP using either a two-point or single-point feed technique. To have CP, two linearly polarized waves that are spatially orthogonal and have an equal amplitude in degenerative modes are excited with identical feeds located on orthogonal sides of the DRA. The signals on the two feeds should have equal amplitude and be in phase quadrature. Hybrid coupler, Wilkinson and T-junction splitters are used to couple the feed to DRA. Leung et al. (2000) achieved CP by microstrip hybrid coupler and conformal strip. The entire 20% axial ratio(AR) bandwidth achieved is not in -10dB impedance bandwidth. Feed structure is also complex. Zou et al. (2013) achieves 18.7% ARBW by traveling-wave excitation. Lumped element resistor loaded spiral slot have been used to excite square DRAs to have wider AR bandwidths. Motevasselian et al. (2013) used copper tape wound around CDRA in a helical shape

and excited by coaxial cable to obtain CP. Zou and Pan (2014) used a modified cross-slot to excite square DRA. The resonance of the cross-slot is merged with DRA for wide ARBW. Patel et al. (2015) high aspect ratio DRAs have been exploited for AR bandwidth improvement. Two CP DRAs are designed by perturbation technique with 41% and 24.6% of ARBW with -10dB impedance bandwidth of 48% and 11.5% respectively. Diagonal four slots and two slots are made in square DRA to widen the ARBW. Wang and Wong (2014) proposed rotate stack technology to broaden AR bandwidth which involves complexity in placing the DRA. They used two rectangular dielectric layers stacked with a rotated w.r.t bottom layer to create a rotated-stair configuration with 31% impedance bandwidth and 18.2% ARBW with 4.5dBi gain. Two RDRA of different dimensions are used. Placing one RDRA on another RDRA is difficult because of the alignment problem. Two adjacent RDRAs create a horizontal stair-shaped configuration. A tall metallic trapezoidal patch is used to excite the DRA to have CP ARBW of 22% from 5.2GHz to 6.5GHz with a gain of 5.7dBi and impedance bandwidth of 37% from 4.6GHz to 6.7GHz was proposed by Fakhte et al. (2015). Varshney et al. (2016) made use of RDRA and two half split CDRA excited by a stair-shaped slot. Impedance bandwidth of 49.67% and AR bandwidth of 41% is obtained. Kumar et al. (2019) has achieved CP in RDRA by only modifying the feed and ground slot. Dual-mode wideband CP RDRA is implemented by stair shaped microstrip feed line and a pair of L-shaped slots in the ground. The measured impedance bandwidth of 26.84% from 2.94Ghz to 3.85GHz and ARBW of 17.59% from 2.96GHz to 3.53GHz. Sun et al. (2018) use the stacked DRA concept to have wide ARBW. 28%(4.85 to 6.1GHz) of ARBW and 25.4%(4.8 to 6.2GHz) impedance bandwidth are obtained. Stacked DRA involves fabrication complexity with an increase in DRA dimension. Zainud-Deen et al. (2019) has proposed a technique to convert LP to CP by using a metamaterial(MM) surface on top of LP DRA. A MM polarizer is placed at a distance from wideband LP DRA, which introduces 17.5% of CP bandwidth.

Circular polarization is achieved by modification in feeding method to DRAs, by using extended patches, conformal strip and slot modification. The perturbation technique is used to achieve CP in DRAs, with new geometric shapes and stacking DRAs

with different dielectric permittivity.

2.3.3 Multiband CP DRAs

In Fang and Leung (2012) dual fed dual band CP CDRA has been achieved by exciting higher orders modes HEM_{111} and HEM_{113} modes with 3dB AR bandwidth of 12.4% and 7.4% involving complex feeding network. San Ngan et al. (2012) used single fed to have dual band CP with chamfered DRA excited with TE_{111} and TE_{113} modes excited with 3dB AR bandwidth of 5.2% and 1.4% for the lower and upper bands. Improved results in 3dB AR bandwidth are proposed by Fang et al. (2014); Pan et al. (2014) of 6.3% and 3.68%, 3.16% and 5.06% respectively. Zhou et al. (2015) had a modified CDRA, excited with HEM_{111} and $HEM_{11\delta}(2 < \delta < 3)$ by microstrip to obtain dual band CP with impedance bandwidth of 26.25%(4.6 to 5.99GHz) and 11.17%(8.54 to 9.55GHz) and 3dB AR bandwidth of 15.8%(4.78 to 5.6GHz) and 5.02%(8.94 to 9.4). Zou and Pan (2015) have achieved wide axial bandwidth of 20% by merging two similar modes with the resonant frequency of the stacked structure and by adopting cross-slot coupling. Dual band CP less than 3dB ARBW of 9.7% and 20% band ranges from 1.76 to 1.94GHz and 2.39 to 2.92GHz and impedance bandwidth of 12.2%(1.77-2GHz) and 21.7%(2.38-2.96GHz). Stacked RDRA is used, which increases the dimension. Varshney et al. (2018) use an inverted sigmoid shaped DR and a metallic strip at the surface of the DR to achieve dual band CP. The fundamental and higher order hybrid modes are excited in the DRA with a 3dB AR bandwidth of 19.98% and 3.07%.

Most of the work done in achieving multiband CP is by hybrid technique(i.e. resonating slot and DRA for different frequencies) or exciting higher order modes and fundamental mode by modification in feed, DRA geometry and stacked DRAs.

2.3.4 Frequency reconfigurable DRAs

Diversity antennas have become very popular in modern wireless communication because they reduce the fading effect and increase channel capacity. Pattern reconfig-

urable antennas produce more than one radiation pattern with different directivity. The manipulating patterns help avoid noise, mitigate electronic jamming, improve security, and increase energy efficiency. Traditionally two or multiple antennas have been used to provide different radiation patterns. Such design increases the overall antenna size and the feed network's complexity. Reconfigurable antennas are attractive in applications such as multiple-input multiple-output (MIMO), mobile terminals, cognitive radio communications, surveillance and tracking. The antenna with reconfigurable characteristics can be used to provide a variety of functions by modifying its operating frequency, beam patterns and polarization dynamically. An antenna with a reconfigurable frequency can switch to the desired frequency instead of utilizing several antennas operating at different frequencies. The frequency reconfigurable antenna provides multi-frequency operation in a single antenna with improved performance and reduces space and cost. Dynamic tuning can be achieved by switching mechanisms through controlling mechanical, electronic, physical, or optical switches. Different techniques have been investigated in various wireless communication systems. The electronic switches are the most prominent used in reconfigurable antennas due to their efficiency, reliability and ease of integration. The electrical reconfiguration uses positive–intrinsic–negative (PIN) diodes, varactors and radiofrequency micro-electromechanical system (RF MEMS) switches. PIN diodes have good performance and a low price compared to RF MEMS switches. Yan and Bernhard (2011) has been achieved pattern diversity by exciting $HEM_{11\delta}$ and $TE_{011+\delta}$ in a split elliptic DRA. TE_{111} and quasi-TM_{111} modes are excited in cross-shaped RDRA by Zou and Fumeaux (2011) to have pattern diversity. Pattern diversity has been obtained with $TM_{01\delta}$ and $HEM_{12\delta}$ by Yang and Leung (2019). To make two resonance frequencies equal a meanderline loaded annular slot is used. Various frequency tuning techniques have been proposed in the literature (Desjardins et al., 2012; Pendharker et al., 2014; Apperley and Okoniewski, 2014). In Desjardins et al. (2012) two conducting walls are used on opposite vertical faces of the DRA, which are switched via conducting tabs to be in contact or not with the ground plane for frequency tuning. In Mun et al. (2014), two PIN diodes are used with proximity-coupled feeding. Different states of the diodes allow tuning of the antenna's operating

frequency to cover both LTE 17/13 and LTE 20/7. A frequency tuning between 1.60 GHz and 2.71 GHz is achieved in Danesh et al. (2014). A rectangular dielectric resonator antenna consists of four identical resonators, with three PIN diode switches on the feed line network between each pair of resonators. In Danesh et al. (2013) designed the antenna to operate in either single band or wideband with the two PIN diodes.

Frequency reconfiguration is achieved by different switching techniques. The most commonly PIN diode is used. The mechanisms for reconfiguration must not increase the complexity of the antenna design in terms additional components such as diodes and biasing circuit.

CHAPTER 3

TRIBAND DIELECTRIC RESONATOR ANTENNAS

This chapter discusses triband cylindrical dielectric resonator antenna with an aperture coupled. A linearly polarized cylindrical DRA with designed with a triangular aperture that excites three hybrid modes in the three impedance bands. The $HEM_{11\delta}$, $HEM_{21\delta}$ and $HEM_{13\delta}$ hybrid modes are excited at different frequencies. The diversified radiation pattern is also obtained in different operating frequency bands. $HEM_{11\delta}$ radiates like magnetic dipole and $HEM_{21\delta}$ radiates like magnetic quadrupole. The antenna is designed in regular cylindrical DRA and simple feed to obtain higher order hybrid modes. The antenna performance is validated experimentally by considering impedance bandwidth, gain and radiation pattern.

3.1   Triband Cylindrical Dielectric Resonator Antenna

The triband linearly polarized cylindrical DRA is shown in Figure 3.1. The dielectric resonator antenna is a Roger's TMM10i has a permittivity ϵ_r=9.8, loss tanδ=0.0022, radius r=10mm and height h=6.35mm. The cylindrical DRA is mounted at the center of the ground plane of size 50mm x 50mm. The cylindrical DRA is supported with a substrate FR-4 with permittivity ϵ_r=4.3, tanδ=0.0025 and height hs=0.8mm. The bottom side of the substrate is printed with a microstrip feed line of width w_s and length l_f. The cylindrical DRA is excited by an equilateral triangular slot at the center on the ground of sides 10.39mm.

The selection of feed point and its location determines which modes are excited. This, in turn, determines the input impedance and radiation characteristics of the DRAs. Aperture coupling has the feed network located below the ground plane and isolates the
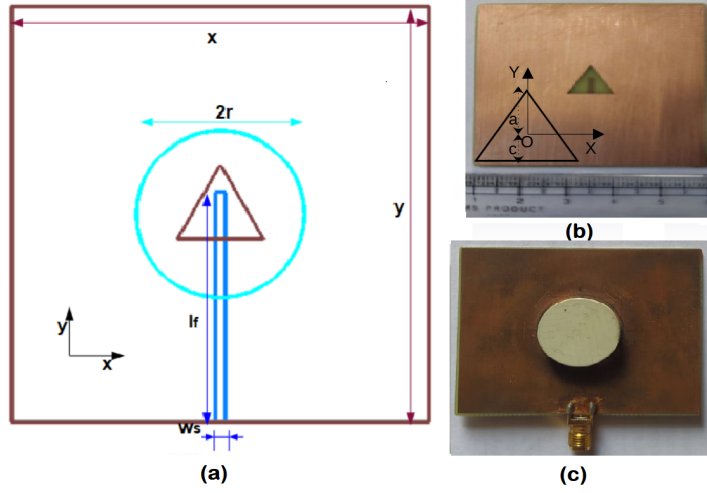
Figure 3.1: (a)Top view of all the layers of the proposed triband cylindrical DRA. Fabricated prototype antenna (b)triangular slot on the ground plane (c)top view. w_s=1.2mm and l_f=31.48mm

radiation aperture from any unwanted coupling from the feed. The source must be located in an area of strong magnetic fields to achieve strong coupling using a magnetic current. A rectangular slot acts as a magnetic current source and is commonly used to excite the $HEM_{11\delta}$ mode in the cylindrical DRA. The slot length "b" and width is calculated using equation 2.3 and 2.4. The rectangular slot is modified to equilateral triangular with same slot length which excites other higher order modes with the fundamental mode $HEM_{11\delta}$. The analysis of the triangular slot on the resonance frequencies was done and shown in Figure 3.2 in terms of "b" base length (slot length) and height "$a + c$", c represents the base distance and a represents vertex distance from the center of the slot. Lesser the value of "a" and "c" results in higher frequency resonance. The value of "c" mainly effects the fundamental resonance. The base length "b" main effects the resonance frequency bands. The feed length was optimized to produce a good impedance match to all the three frequency bands.

The theoretical resonance frequency of $HEM_{11\delta}$ for the specified cylindrical DRA dimension is 4.97GHz, calculated using equation 2.5. The $HEM_{21\delta}$ mode is approximately estimated at 6.52GHz from equation 2.6. A new higher order mode $HEM_{13\delta}$ is also obtained without any change in the antenna dimension with an aspect ratio $\approx$ 0.6. The non-resonant triangular slot with microstrip feed excites three hybrid modes

$HEM_{11\delta}$ at 4.36GHz, $HEM_{21\delta}$ at 6.5GHz and $HEM_{13\delta}$ at 8.89GHz.

(a)

(b)

(c)

(d)
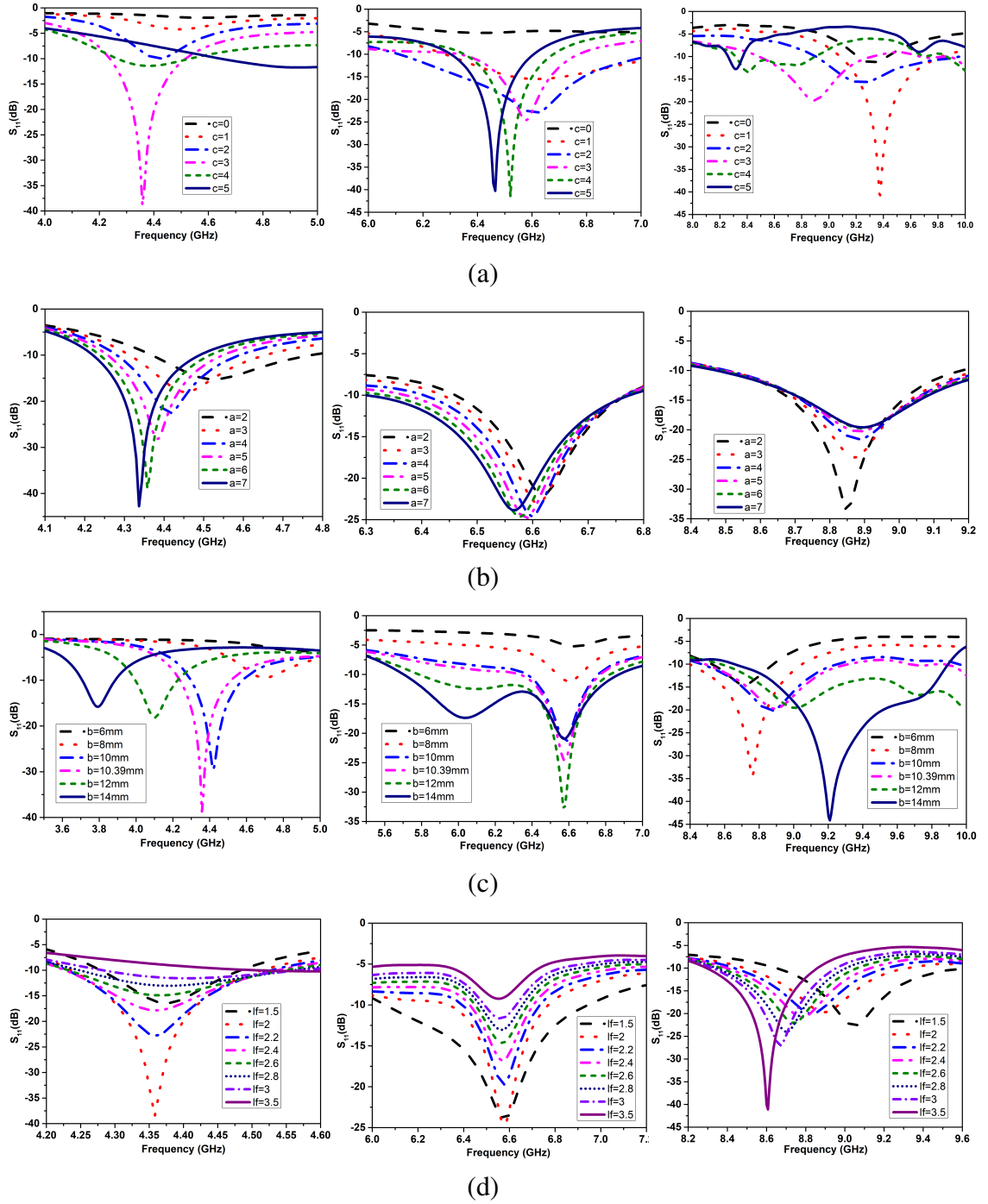
Figure 3.2: Reflection coefficient variation of the proposed triband CDRA with respect to parameter (a)c (b)a (c)b (d)l_f.

The surface current distribution on the triangular slot at the resonance frequency is shown in figure 3.3. The surface current at the base triangular slot are in opposite direction at 4.4 GHz and 6.5 GHz which indicates coupling of HE and EH modes. And

the surface current at 8.8 GHz is similar to 4.4 GHz, excites higher order of HE mode.
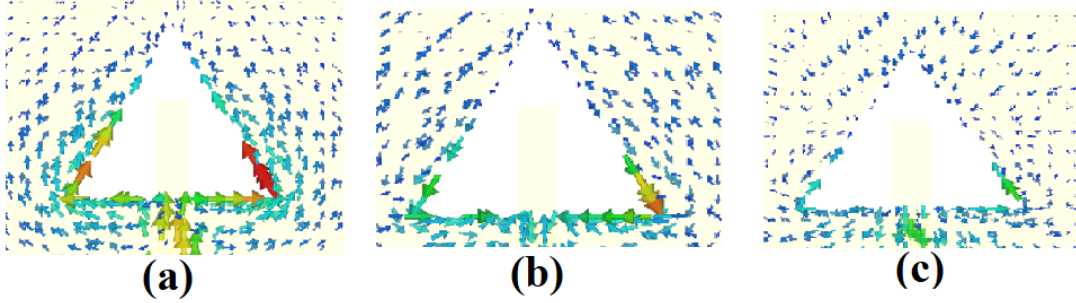
Figure 3.3: Surface current on the triangular slot at (a)4.36GHz (b)6.56GHz (c)8.8GHz.

3.1.1 Fabrication and experimental results

Figure 3.4 shows the contour and near field distribution at 4.36GHz, 6.56GHz and 8.89GHz. From the near field distribution at 4.36GHz and 6.56GHz, the modes are easily recognized as $HEM_{11\delta}$ and $HEM_{21\delta}$ respectively Kajfez et al. (1984). The third mode is identified as $HEM_{13\delta}$ mode and named using the nomenclature as in Kajfez et al. (1984).

The measured results of the antenna S_{11} were obtained using Agilent Technologies E8363C PNA network analyzer. The AR and far field radiation pattern measurements were done using a high-gain horn antenna as a reference antenna and the proposed antenna as a test antenna. Figure 3.5a shows simulated and measured results of S_{11} of the proposed triband cylindrical DRA. The simulated impedance bandwidth (S_{11} <10dB) in the first, second and third bands were 6.62% (4.23-4.52 GHz), 6.87% (6.32-6.77 GHz), and 9.55% (8.47-9.32 GHz) respectively and measured impedance bandwidth were 4.38% (4.24-4.43 GHz), 6.81% (6.38-6.83 GHz) and 15.5% (8.26-9.65GHz) respectively. Simulated and measured gain of 5.7 dBi and 5.4 dBi at 4.4 GHz, 8.2 dBi, and 8 dBi were observed at 8.89 GHz, respectively (Figure 3.5b). A high gain was observed at higher-order mode $HEM_{13\delta}$.

The simulated and measured radiation patterns in the xz and yz planes are shown in figure 3.6-3.8. At 4.3 GHz $HEM_{11\delta}$ mode is exciting results in broadside radiation
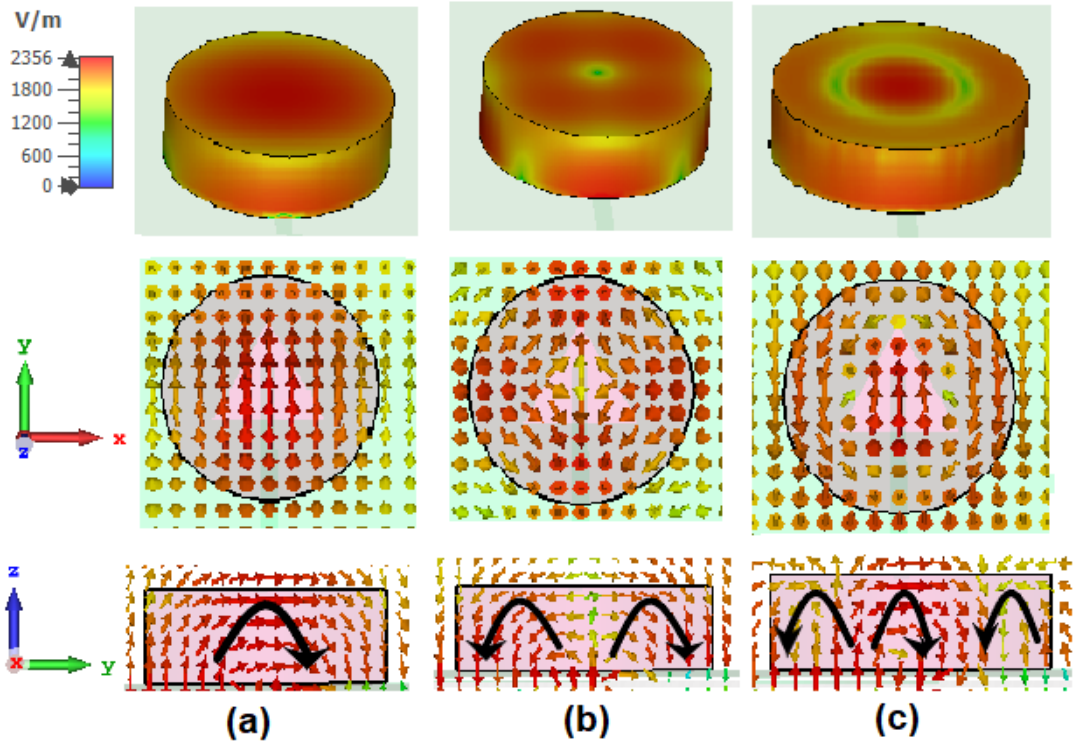
Figure 3.4: Contour and electric field distribution of the proposed triband CDRA in xy and yz plane at (a)4.36GHz (b)6.56GHz (c)8.89GHz
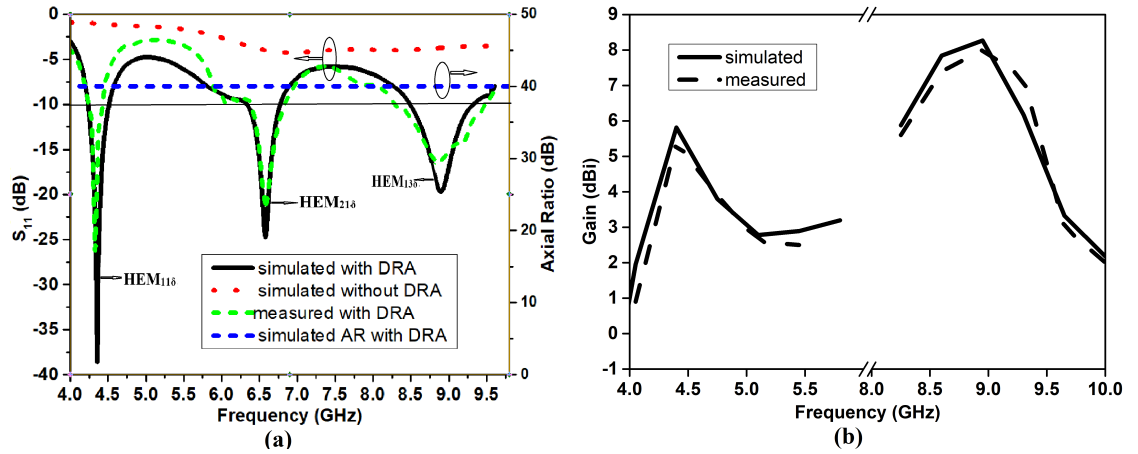
Figure 3.5: Simulated and measured (a)Reflection coefficient and axial ratio (b)Gain of the proposed triband CDRA

and $HEM_{13\delta}$ is a higher mode of $HEM_{11\delta}$also results in broadside radiation. $HEM_{21\delta}$ results in quadrupole radiation. Due to unsymmetrical field distribution in the far-field region, a high gain was observed at $\theta = 36^0$ with 4.9 dBi.
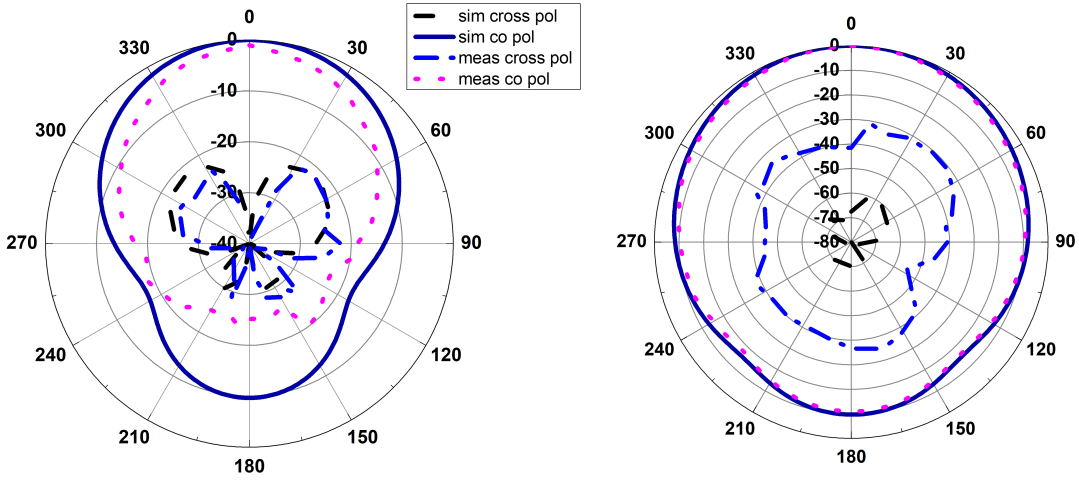
Figure 3.6: Simulated and measured results of the normalized radiation patterns of the proposed triband CDRA at 4.4GHz.
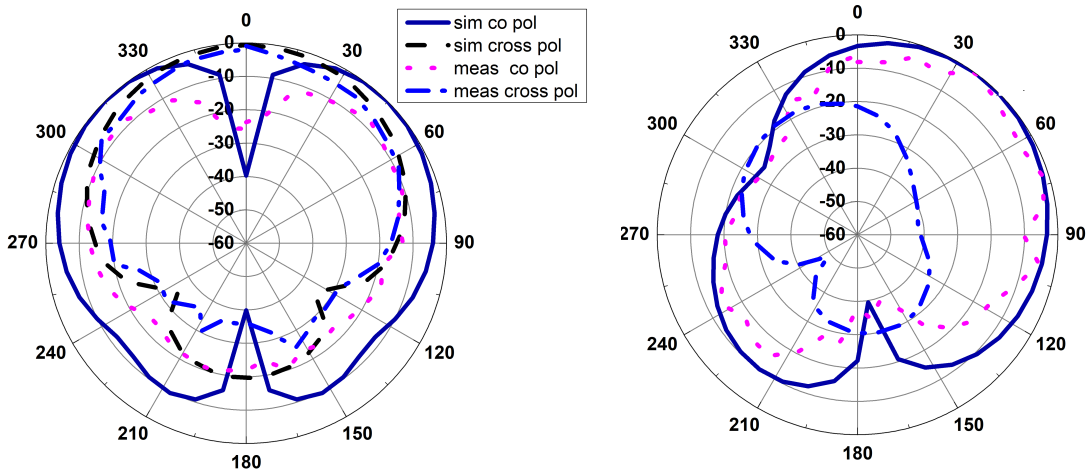
Figure 3.7: Simulated and measured results of the normalized radiation patterns of the proposed triband CDRA at 6.5GHz.

3.1.2 Summary

In this chapter, a triband hybrid radiating LP cylindrical DRA is presented. The hybrid modes are achieved using a novel triangular aperture slot. A new $HEM_{13\delta}$ mode is excited with a simple aperture without suppressing fundamental mode $HEM_{11\delta}$ and weak mode $HEM_{21\delta}$. The antenna gives different radiation patterns.
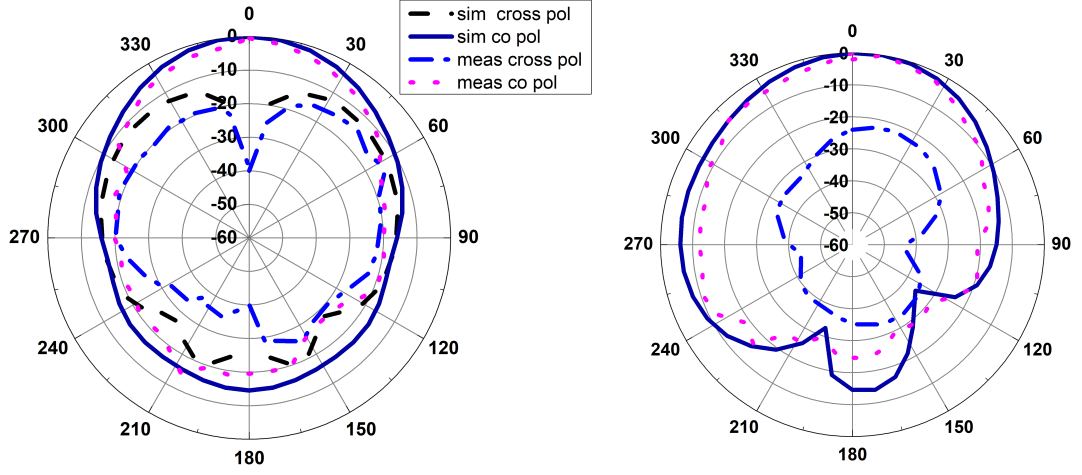
Figure 3.8: Simulated and measured results of the normalized radiation patterns of the proposed triband CDRA at 8.8GHz.

Table 3.1: Comparison of present work with earlier reported work (DRA $\epsilon_r \approx 10$).

Feed configuration	Modes	Resonate Freq (GHz)	Impedance bandwidth	Peak Gain (dBi)	DRA vol (mm^3)
Cross shaped composite aperture Guha et al. (2015)	$HEM_{11\delta}$ $HEM_{12\delta}$	3.9 7.4	7% 8%	5.6 6	3142
Twin aperture Gupta et al. (2021)	$HEM_{11\delta}$ $HEM_{111+\delta}$	3.85 7.85	10% 10%	6.3 9	3142
Triangular aperture [Present LP CDRA]	$HEM_{11\delta}$ $HEM_{21\delta}$ $HEM_{13\delta}$	4.36 6.56 8.89	4.3% 6.81% 15.5%	5.7 3.9 8.2	1995

CHAPTER 4

CIRCULARLY POLARIZED DIELECTRIC
RESONATOR ANTENNAS

Circularly polarized (CP) antennas are preferable over linearly polarized (LP) antennas because of their orientation, resistance to polarization losses, immunity to Faraday's rotation effect, fading channels, multipath interference, and environmental effects. Wireless communication requires CP antennas to overcome these problems. This chapter presents circular polarization in cylindrical and rectangular dielectric resonator antenna using aperture feed.

In the first section, a CP cylindrical DRA is obtained by a triangular aperture and a flag shaped microstrip. The antenna has three impedance bands with six different hybrid radiating modes and three CP bands. The antenna can be used in both C and X band frequency applications. An elliptical slot aperture is used to feed rectangular DRA is discussed in the second section. The nonresonant elliptical slot excites two orthogonal modes to provide CP. The sense of polarization can be controlled by changing the orientation of the elliptical slot. The third section presents a wide axial ratio beamwidth with a metallic strip loaded rectangular dielectric resonator antenna.

4.1 TRIBAND CIRCULARLY POLARIZED CYLINDRICAL DIELECTRIC RESONATOR ANTENNA

4.1.1 Antenna structure and Its operation

The triband LP CDRA discussed in chapter 3 is used to provide circularly polarized bands with modified feed without changing the dielectric resonator geometric and triangular aperture slot. The flag shape microstrip feed generates additional hybrid radiating modes $HEM_{21\delta}$-like, $HEM_{12\delta}$, and $HEM_{14\delta}$ resulting in six different modes. Three CP bands are obtained in the third impedance band. Figure 4.1 shows the top view of the antenna with different layers and a fabricated prototype of the top and bottom layers of the substrate. The resonance due to weak coupling ($HEM_{12\delta}$ and $HEM_{14\delta}$) of triband LP CDRA are made to resonate. The feed modification has enhanced the S_{11} bandwidth and changed the axial ratio response.

4.1.2 CP Waves Creation

It is well-known that CP waves are created by the same amplitude orthogonal component of an E-field. A flag shape patch along with the feed line generates CP hybrid mode. Hybrid modes are generated in CP CDRA because of imperfect PEC and PMC boundary conditions. Hybrid modes are degenerative modes. Default hybrid modes are degenerative modes. The hybrid modes are divided into HE and EH modes. HE_{m+1n} and EH_{m-1n} modes are generally degenerate. And coupling between the EH and HE modes changes their polarization state and field configuration. There exists a multipole corresponding to each degenerate hybrid mode. For example, $HEM_{11\delta}$ mode radiates a magnetic dipole along the radial direction and $HEM_{21\delta}$ mode radiates like a magnetic quadrupole along the transverse direction.
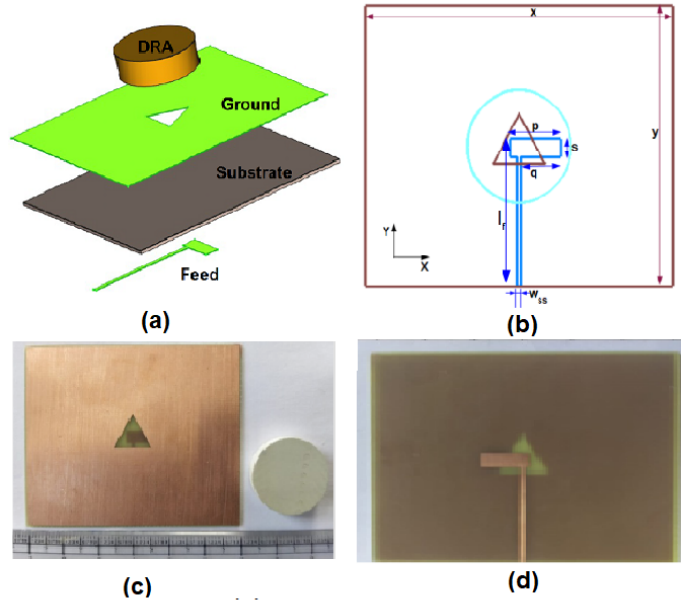
Figure 4.1: (a)3D view of different layers of the proposed CP CDRA (b)Top view of the proposed CP CDRA with all the layers. Fabricated prototype of the proposed CP CDRA (c)Triangular slot on the ground plane (d)Bottom view of the substrate. x = 60, y = 50, r = 10, w_{ss} = 1.2, l_f = 31.48, p = 9.8, q = 8 and s = 3.48 (all dimensions are in mm).

4.1.3 Fabricated design and Results

The CP cylindrical DRA was fabricated to validate the simulated results. The feed parameters p, q, s, l_f, and w_{ss} were optimized to obtain the triband CP band. The near field electric distribution was used to identify the hybrid radiating mode of $HEM_{11\delta}$, $HEM_{21\delta}$-like, $HEM_{21\delta}$, $HEM_{12\delta}$, $HEM_{13\delta}$ and $HEM_{14\delta}$, generated at 4.68 GHz, 6.23 GHz, 6.66 GHz, 8.45 GHz, 9.12 GHz, and 9.74 GHz. The electric field distribution of $HEM_{12\delta}$ and $HEM_{14\delta}$ are shown in Figure 4.2. Figure 4.3a shows simulated and measured results of S_{11}. An additional resonance frequency was observed at 6.23 GHz, which is the slot resonance. The verified theoretical resonance frequency of the triangular slot is 6.14 GHz (Garg et al., 2001). The simulated first band is 4.38-4.99 GHz (13.02%), the second band 5.95-7.12 GHz (17.90%), and the third band 8.05-9.79 GHz (19.51%). The measured impedance bands were 4.23-4.53 GHz (6.84%), 5.95-6.91 GHz (14.93%), and 7.69-9.95 GHz (25.62%), respectively. A high gain was obtained in the third impedance band. The simulated and measured gain at 4.7 GHz

and 8.7 GHz were 5.7 dBic, 5.6 dBic, 7.5 dBic, and 7 dBic respectively at $\phi = 0^0$ and $\theta = 0^0$. At 6.5 GHz radiation beam is tilted due to $HEM_{21\delta}$ mode and the maximum simulated gain of 5 dBic is obtained at $\theta = 36^0$.

(a) **(b)**
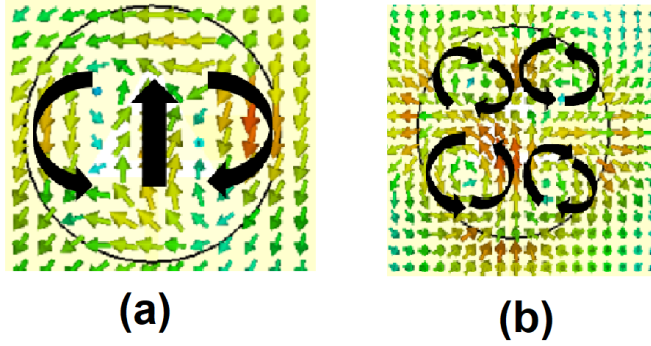
Figure 4.2: Electric field distribution in the xy plane at (a)8.45 GHz and (b)9.74GHz.
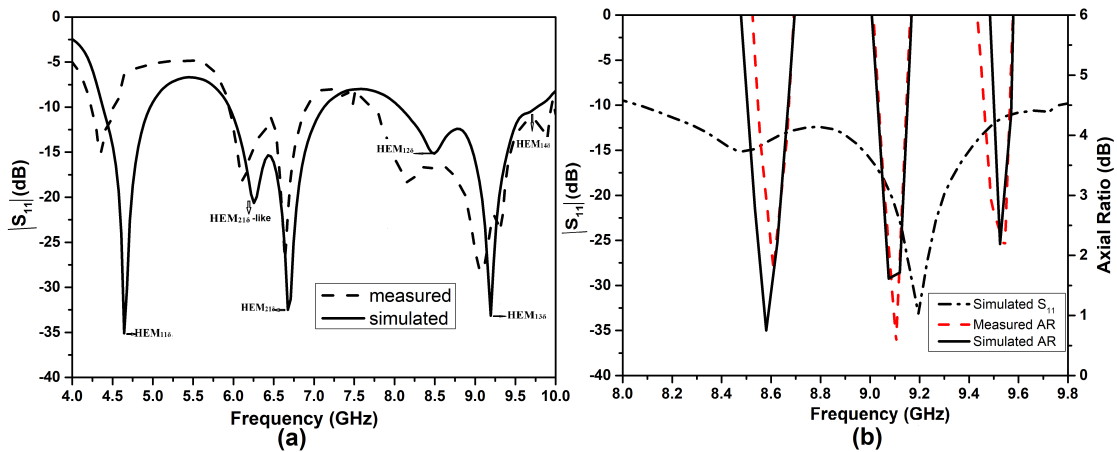
Figure 4.3: Simulated and measured results of the proposed CP CDRA (a)S_{11} (b)Axial ratio.

Figure 4.3b shows simulated and measured axial ratio (AR) response results. The measured 3 dB AR bandwidth in the third impedance band were 8.53-8.64 GHz (1.28%), 9.05-9.15 GHz (1.09%) and 9.48-9.56 GHz (0.84%), and simulated values were 8.52-8.64 GHz (1.39%), 9.03-9.14 GHz (1.21%) and 9.15-9.54 GHz (0.315%). The simulated electric field distribution is analyzed at different resonance frequencies in the +z direction in the xy plane of the CP cylindrical DRA. The electric field distribution at different CP bands is shown in the figure 4.4-4.5. It is observed that clockwise rotation of E-field at 8.6 GHz, 9.1 GHz and 9.5 GHz. Hence, right-hand circular polar-

ization (RHCP) is obtained. One more CP at 4.3 GHz with $S_{11} \approx$ -9dB was observed with an AR bandwidth of 4.34-4.38 GHz. Since the value of S_{11} is not less than -10dB the result is not presented here. And the anticlockwise rotation of the E-field is observed at 6.5 GHz, indicating left-hand circular polarization (LHCP). The state of polarization changes due to $HEM_{21\delta}$ modes which is EH mode. The result is not presented here since the gain at 6.5 GHz is maximum at not $\theta = 0^0$. Further analysis can be done to achieve CP bands in the first and second impedance bands. The far-field of the CP cylindrical DRA was obtained using with single horn antenna (Wang et al., 2017). Figure 4.6-4.8 show the measured and simulated radiation pattern in the boresight direction at the CP band frequencies. A good separation between LHCP and RHCP fields is observed in both the xz and yz planes. Table 4.1 provides the comparison between the existing literature and the worked CP cylindrical DRA.

(a)

(b)
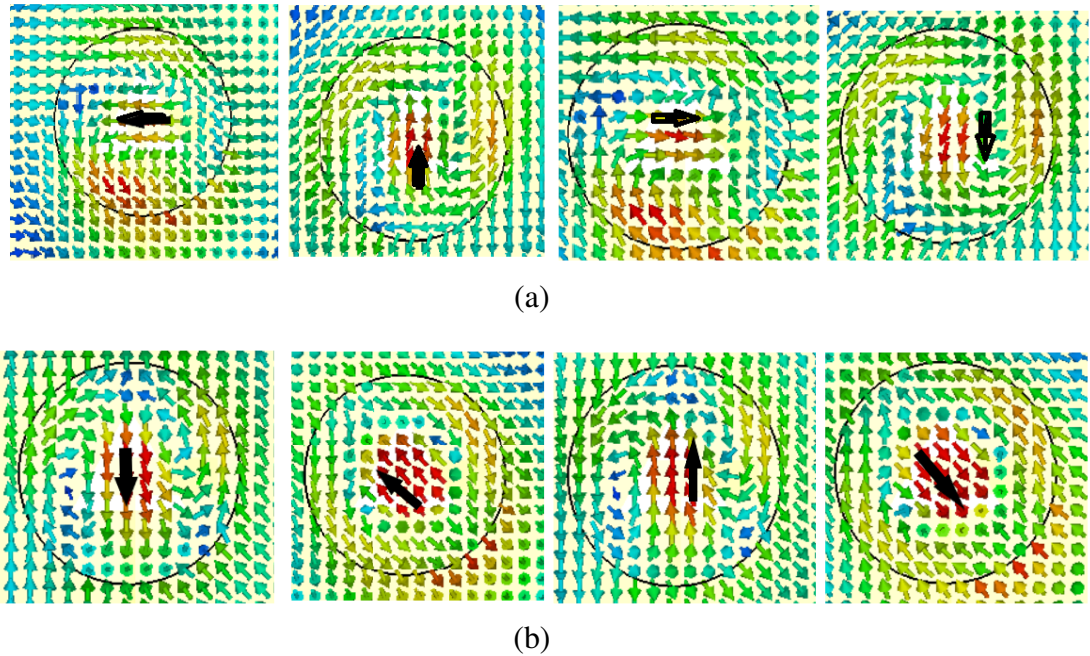
Figure 4.4: Electric field distribution at time instant of t=0, T/4, T/2 and 3T/4 at (a)8.6 GHz (b)9.1 GHz (c)9.5 GHz (d)6.5 GHz.
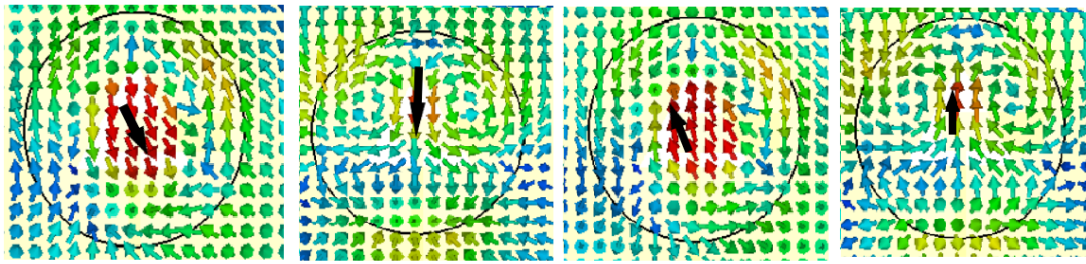
(c)
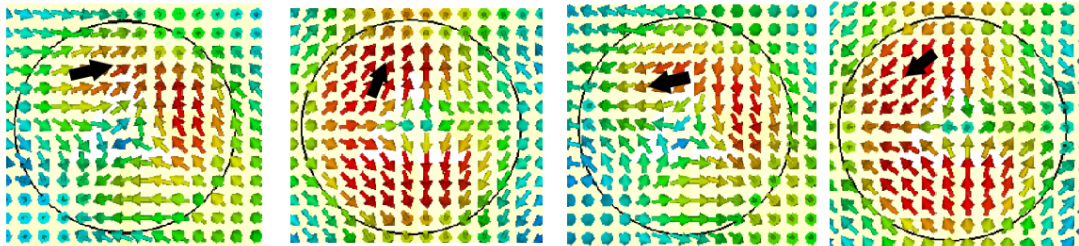
(d)

Figure 4.5: Electric field distribution at time instant of t=0, T/4, T/2 and 3T/4 at (a)8.6 GHz (b)9.1 GHz (c)9.5 GHz (d)6.5 GHz.
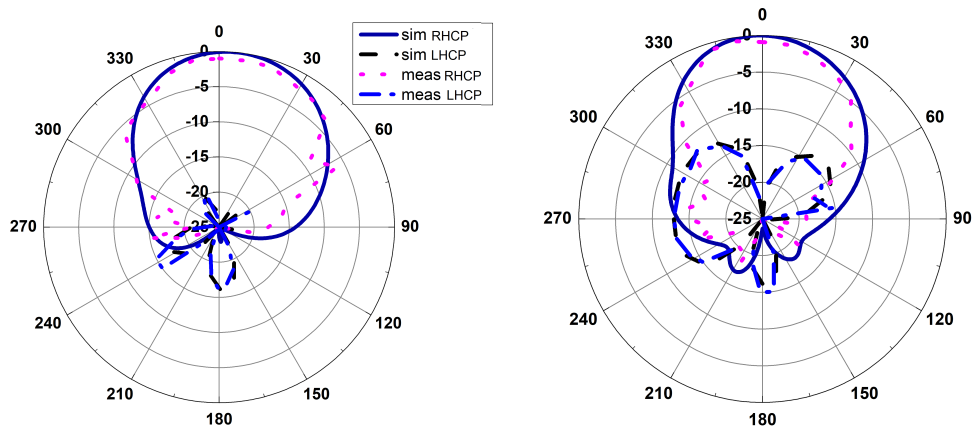
(a)

Figure 4.6: Simulated and measured results of normalized radiation patterns of the proposed CP CDRA in the xz and yz plane at (a)8.6 GHz (b)9.1 GHz (c)9.5 GHz.
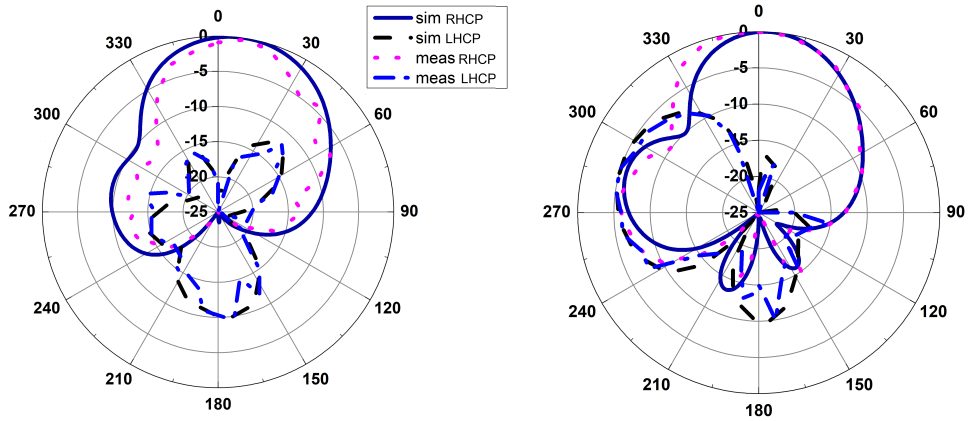
(b)

Figure 4.7: Simulated and measured results of normalized radiation patterns of the proposed CP CDRA in the xz and yz plane at (a)8.6 GHz (b)9.1 GHz (c)9.5 GHz.
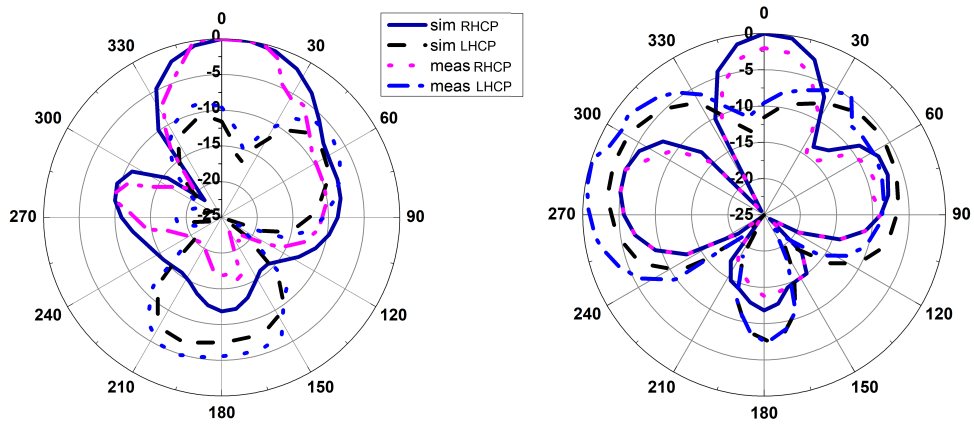
(c)

Figure 4.8: Simulated and measured results of normalized radiation patterns of the proposed CP CDRA in the xz and yz plane at (a)8.6 GHz (b)9.1 GHz (c)9.5 GHz.

4.2 Circularly Polarized Rectangular Dielectric Resonator Antenna with Elliptical Aperture Feed for 5GHz ISM band

This section presents a new elliptical slot aperture feed circularly polarized rectangular DRA. The nonresonant slot excites two spatially orthogonal resonant frequencies in

Table 4.1: Comparison of present work with earlier reported work (DRA $\epsilon_r \approx 10$).

Feed configuration	Modes	Resonate Freq (GHz)	Impedance bandwidth	CP band-width	Peak Gain (dBi)	DRA vol (mm^3)
Strategic shaped aperture with cross-shaped microstrip feed Sharma et al. (2020)	$HEM_{11\delta}$ $HEM_{111+\delta}$ $HEM_{12\delta}$-like + $HEM_{12\delta}$ + $HEM_{13\delta}$ $HEM_{14\delta}$	1.1 1.57 2.28 2.6	0.97-1.2 1.46-1.2 1.89-2.48 2.55-2.96	11.65 7.64 7.01 7.1	5	127000
Inverted pentagon-shaped with quarter annular stub loaded feed-line Sharma et al. (2017b)	$HEM_{11\delta}$ $HEM_{11\delta}$+ $HEM_{12\delta}$	2.6 5.5	2.58-2.96 4.83-5.93	- 8.78	5.5 6.2	6902
Triangular aperture with flag-shaped microstrip feed [Present CP CDRA]	$HEM_{11\delta}$ $HEM_{21\delta}$-like + $HEM_{21\delta}$ $HEM_{12\delta}$ + $HEM_{13\delta}$ + $HEM_{14\delta}$	4.68 6.5 9.12	4.23-4.53 5.95-6.91 7.95-9.95	1.28 1.09 0.84	5.7 5 7.5	1995

rectangular DRA to produce circularly polarized (CP) waves. TE_{111}^x and TE_{111}^y are the orthogonal modes produced by the 45^0 inclined elliptical slot with respect to microstrip feed. Also, the sense of polarization at the resonance frequencies can be controlled by changing the orientation of the slot.

4.2.1 Antenna design and working principle

The antenna is designed on Rogers RO4003 substrate ($\epsilon_s = 3.55$ and $\tan \delta = 0.0027$) of 40 mm X 48 mm dimension of thickness 0.8 mm. A w mm X d mm X b mm dimension ceramic material of Rogers TMM10i ($\epsilon_r = 9.8$ and $\tan \delta = 0.0022$) is glued on the copper

ground plane. The ground plane lies on the top layer of the RO4003 substrate and a 50Ω microstrip line of width 2.4 mm and length of 28 mm is etched on the bottom layer of the RO4003 substrate. The antenna with different layers is shown in figure 4.9.
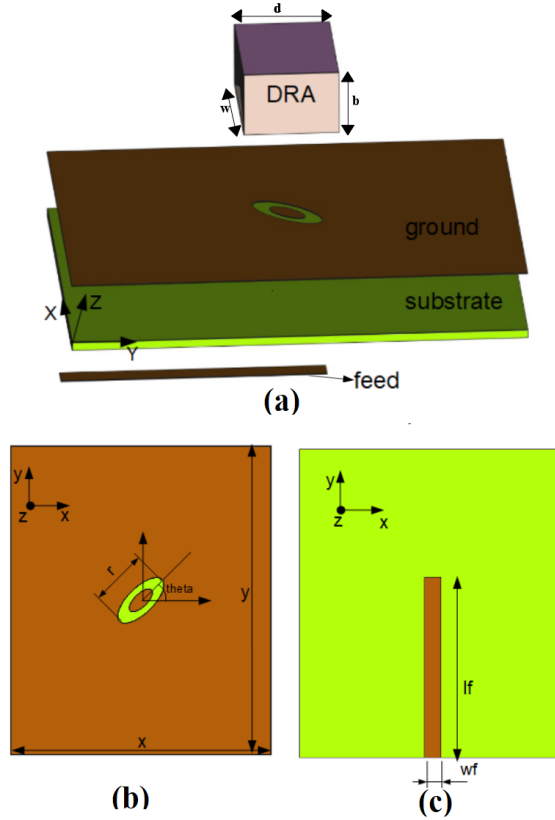
Figure 4.9: (a)3D view of the proposed antenna showing different layers (b) Top layer of the substrate (c)Bottom layer of the substrate. w= 15, d=10, b=6.35, x= 40, y=48, r=4.6, theta=450, l_f=28 and w_f=2.4 (All dimensions are in mm).

4.2.2 CP Generation

TE and TM modes are obtained in an isolated rectangular DRA. In the case of rectangular DRA mounted on the ground plane, only TE modes are typically excited (Mongia and Bhartia, 1994) and to generate CP fields, a pair of orthogonal modes with equal amplitude are to be excited in rectangular DRA. The resonant mode frequencies of isolated rectangular DRA can be predicted using the transcendental equations (2.9)-(2.11) (Petosa, 2007). The estimated mode frequency of TE^z_{111} is 6.3421 GHz. And similarly, TE^x_{111} and TE^y_{111} are obtained at 6.54 GHz and 5.78 GHz, respectively. Rectangular

DRA can easily generate orthogonal modes by properly choosing the excitation.
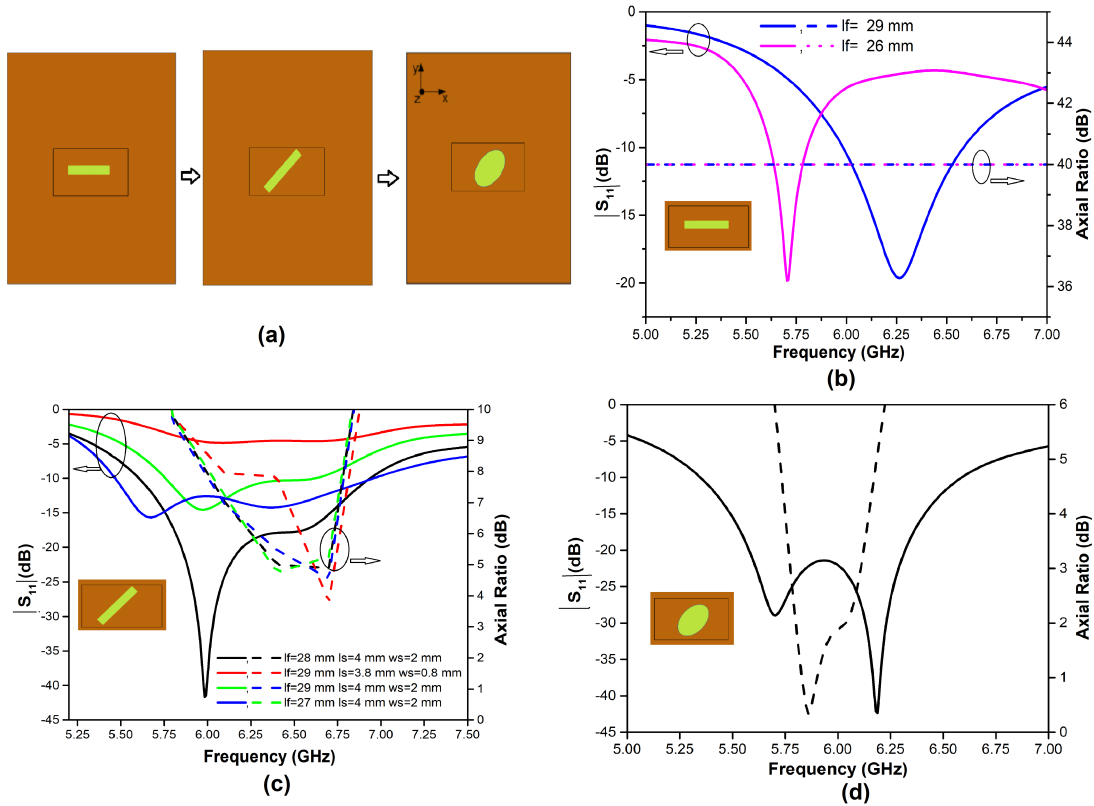
Figure 4.10: (a)Evolution of antenna slot on the ground plane. Simulated S_{11} and axial ratio for different slots shape (b)Rectangular slot (c)Inclined rectangular slot (d)Elliptical slot.

The geometry of the evolution of the proposed elliptical slot on the ground plane to achieve CP is shown in figure 4.10(a). Initially, the most widely used rectangular slot aperture was used to excite the rectangular DRA. The slot length (l_s = 7.6 mm) and slot width (w_s = 0.8 mm) were calculated as in Petosa (2007). CST Microwave Studio simulation software was used to simulate the rectangular DRA. It was observed that rectangular DRA resonates at 5.714 GHz and 6.24 GHz for feed lengths (l_f) of 26 mm and 29 mm with linearly polarized shown in figure 4.10(b). These modes can be used to produce circular polarization by exciting both the modes together with 90^0 phase difference. The quadrature phase is fulfilled when $f1 + \Delta f1/2 = f2 - \Delta f2/2$ where Δf is the 3 dB bandwidth of S_{11} and f1 and f2 are orthogonal (f1< f2) modes. To achieve CP, the rectangular slot was inclined at 45^0 with respect to microstrip feed. The parametric study of feed length, slot width and slot length was done to verify impedance

bandwidth and 3 dB AR. The AR value reduces but resonant frequencies changes (figure 4.10(c)). To obtain the required resonant modes and AR, an inclined rectangular slot is modified into an elliptical slot with a major axis of 4.6 mm and a minor axis of 2 mm. The elliptical patch easily generated CP fields (Jung and Seo, 2002). The slot creates an asymmetry E-fields to generate an orthogonal mode in rectangular DRA. The nonresonant elliptical slot excites fundamental orthogonal modes TE^x and TE^y in rectangular DRA and mergers to radiate a circularly polarized signal. The simulated reflection coefficients and AR with elliptical slot are shown in (figure 4.10(d)). The resonate modes were identified as TE^y_{111} and TE^x_{111} modes from the electric field distribution at 5.7 GHz and 6.2 GHz, respectively (Petosa, 2007) are shown in figure 4.11. To improve the AR bandwidth, the elliptical slot etched on the ground was modified to an elliptical ring slot, as shown in figure 4.9(a). A small elliptical copper patch is placed at the center elliptical slot with the major axis 2 mm. The rectangular DRA with elliptical ring slot also excites the orthogonal TE^y_{111} and TE^x_{111} and mergers to achieve CP. A slight improvement in impedance bandwidth and AR bandwidth was observed compared to the elliptical slot.
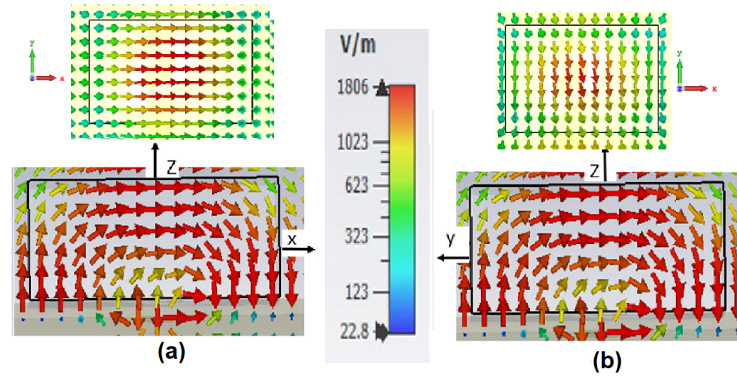
Figure 4.11: Electric field distribution at (a)5.7 GHz (b)6.2 GHz.

4.2.3 Parametric Study

The TE^y_{111} and TE^x_{111} modes were generated simultaneously in the rectangular DRA due to the elliptical ring slot excitation. To study the effect of elliptical ring slot on orthogonal mode pairs excited in rectangular DRA, the feed length l_f, the major axis of

the elliptical ring slot r and the inclined angle theta were varied. The parametric study of these parameters on S_{11} and AR is shown in figure 4.12. From the observation the feed length affects mainly the resonance frequencies rather the axial ratio bandwidth. The major axis of the elliptical slot the affects the excitation of the modes in the resonatoras shown in figure 4.9b. The inclination angle of the elliptical slot with x-axis control the axial ratio bandwidth. At $\theta = 45^0$ maximium axial ratio bandwidth is obtained. An optimized value of l_f = 28 mm, r = 4.6 mm and $\theta = 45^0$ were selected to get improved impedance bandwidth and AR bandwidth.

4.2.4   Simulation and Measured Results

To validate the simulated results of the proposed antenna, a prototype was fabricated and tested (figure 4.13). The -10 dB simulated impedance bandwidth of the antenna was 21.85% (5.34 GHz to 6.65 GHz) and AR bandwidth was 5.88% (5.77 GHz to 6.12 GHz) compared to elliptical slot ground with simulated impedance bandwidth was 19.7% (5.33 GHz to 6.5 GHz) and 3 dB AR bandwidth is 5.7% (5.77 GHz to 6.11 GHz). There is a very small change in impedance and AR bandwidth of the elliptical slot and elliptical ring slot because the excitation of the rectangular DRA is along the circumference of the elliptical slot in both cases. The measured impedance bandwidth of the designed antenna was 23.63% from 5.26 GHz to 6.67 GHz (figure 4.14(a)) and 3 dB AR bandwidth was 6.72% from 5.75 GHz to 6.15 GHz (figure 4.14(b)). In the fabricated prototype of the antenna, the rectangular DRA is manually placed on the ground plane. The challenges are involved in placing rectangular DRA on the ground plane at the required inclination angle with the elliptical ring slot.

The simulated electric field distribution also confirmed the CP at 5.85 GHz for the different instant time intervals are shown in figure 4.15. It is observed from the +z direction that the electric field vector rotates in the anticlockwise direction and produces left-hand CP (LHCP). The gain values were measured and plotted for different frequencies. The measured and simulated gain are shown in figure 4.16. A measured gain of 5.9 dBic and simulated gain of 6 dBic is achieved at 5.85 GHz with more than
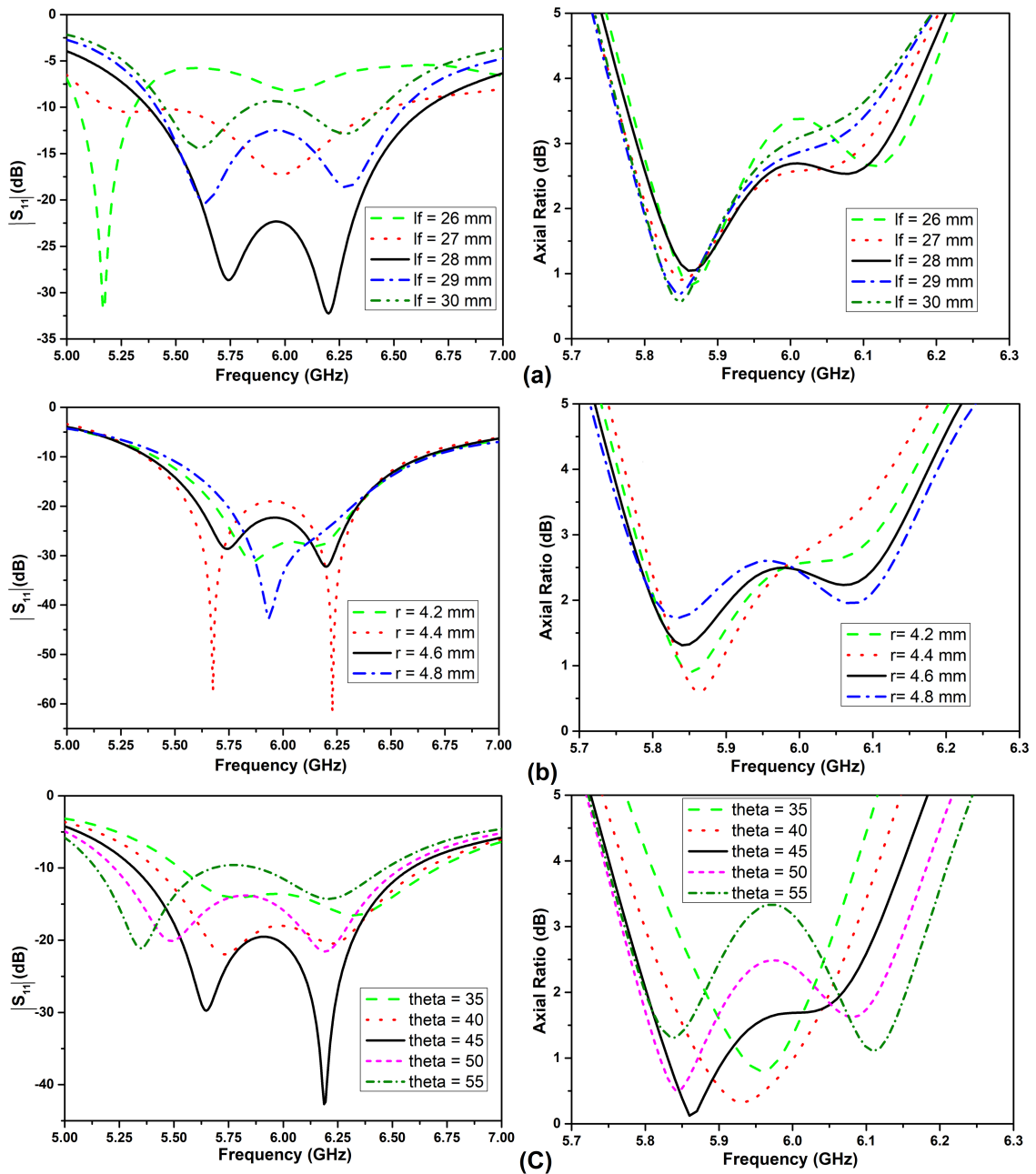
Figure 4.12: S_{11} and axial ratio response when (a)l_f (b)r (c)theta(in degrees) were varied.

95% efficiency. Figure 4.17 shows the simulated and measured radiation pattern at 5.85 GHz. A cross polarization of more than 25 dB in both xz and yz planes is observed at $\theta = 0^0$. Due to TE_{111} excitation, the radiation pattern is in the boresight direction. By changing the orientation of the elliptical ring slot to -45^0 with respect to feeding line/ rectangular DRA right-hand CP (RHCP) can be obtained. Table 4.2 gives a com-
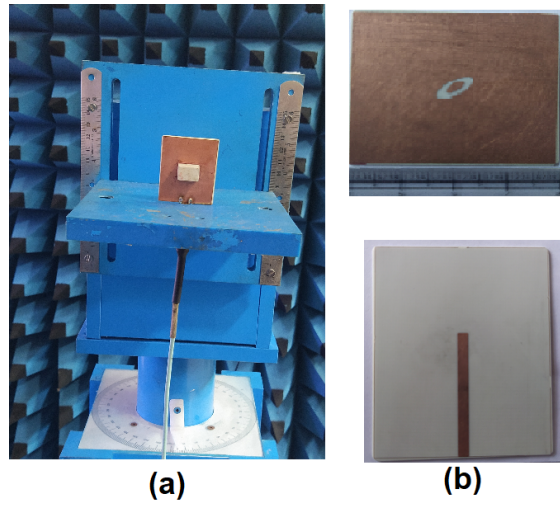
Figure 4.13: (A) Fabricated proposed antenna with measurement set-up (B) Fabricated top and bottom layers of substrate.
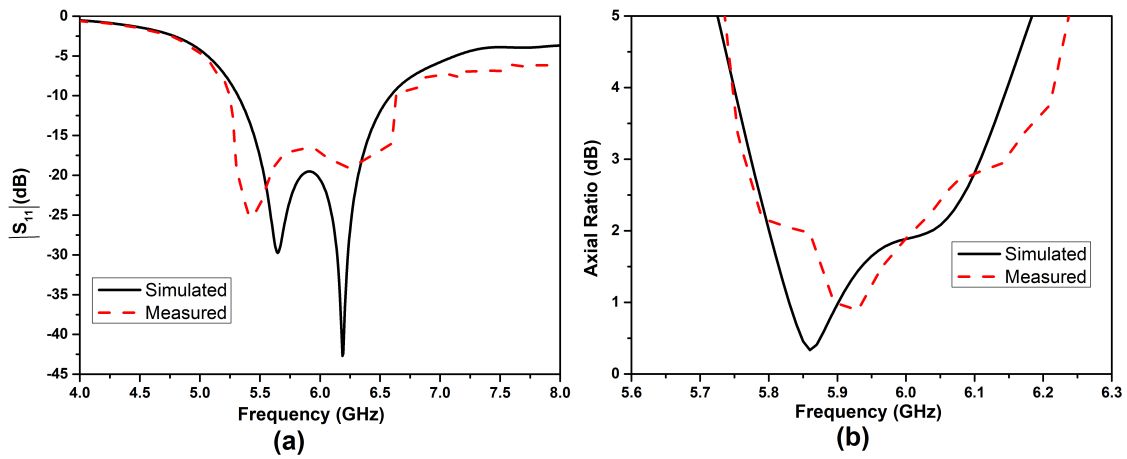
Figure 4.14: Simulated and measured (a)S_{11} (b)Axial ratio.

parative justification based on earlier published work on conventional rectangular DRA with aperture feed. It is observed from table 4.2 new elliptical slot achieves less CP band in the 5GHz ISM band (5.725GHz-5.875GHz) but provides better efficiency and gain compared with previous work with reduced DRA dimension.
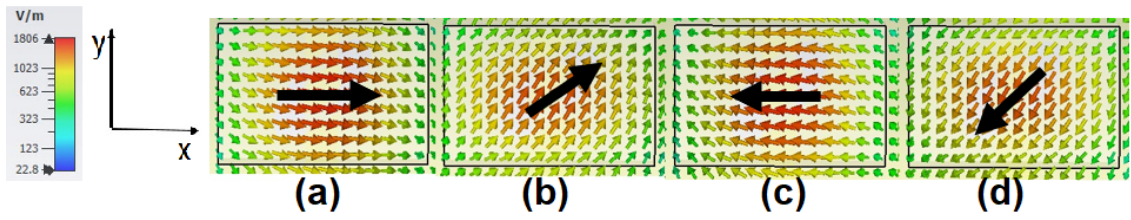
Figure 4.15: Electric field distribution at 5.85 GHz at (A) t=0 (B) t=T/4 (C) t=T/2 (D) t=3T/4.
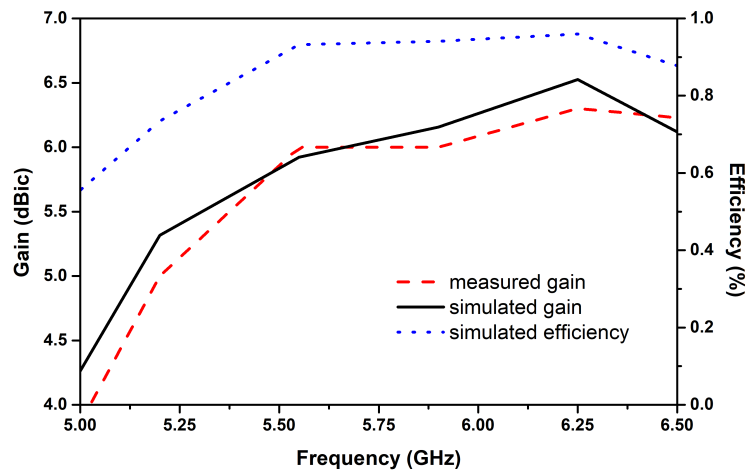
Figure 4.16: Simulated and measured gain and efficiency
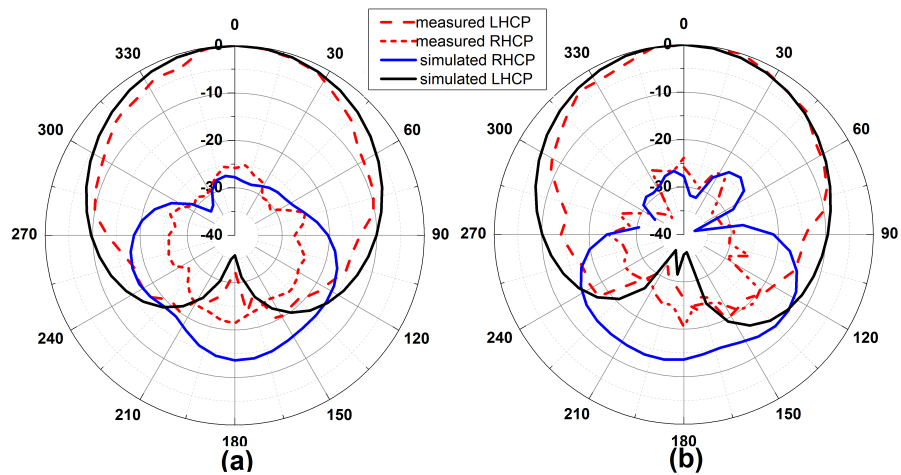
Figure 4.17: Simulated and measured radiation pattern of proposed antenna at 5.85 GHz (A) xz plane (B) yz plane

Reference	$\eta\%$	Gain (dBi)	Slot type	f_O (GHz) (CP)	ϵ_r	V(mm^3)	BW1 (GHz)	BW2 (GHz)	Modes	Change of Polarization
Zou et al. (2013)	75	3.88	Resistance loaded monofilar spiral slot	2.5	12	9000	0.48	1.36	TE_{111}^x and TE_{111}^y	No
Zou and Pan (2014)	95	5	Modified cross-slot	2.5	11	15488	0.63	0.73	TE_{113}^x and TE_{113}^y + slot resonance	No
Zou et al. (2015)	82	4.95	Archimedean sprial	2.13	12	16000	0.57	Na	TE_{111}^x and TE_{111}^y	No
Kumar and Chaudhary (2018b)	92	4.2	F shaped slot	5.32	9.8	5984	0.76	2.75	TE_{113}^x and TE_{113}^y	No
Kumari and Gangwar (2018)	95	4.75	Modified square + ring slot + offset feed	5.5	9.8	10571	0.43	0.5	TE_{121}^x and TE_{211}^y	No
Kumari and Gangwar (2018)	93	4.5	cross slot + spiral feed	3	9.8	8624	0.62	1	TE_{111}^x and TE_{111}^y	Yes
Kumar and Chaudhary (2018a)	84	5.07	plus shaped slot + ring feed	3.37	9.8	6840	0.42	0.68	TE_{111}^x and TE_{111}^y	No
Kumar et al. (2019)	87	4.15	pair of L shaped slots	3.4	9.8	6840	0.57	0.91	$TE_{\delta 11}^x$ and $TE_{1\delta 1}^y$	No
Proposed work	95	5.9	Elliptical	5.85	9.8	945	0.4	1.41	TE_{111}^x and TE_{111}^y	Yes

Table 4.2: Comparison to previous work(BW1-AR bandwidth, BW2-Impedance Bandwidth, V-Volume).

4.3 Circularly Polarized Rectangular Dielectric Resonator Antenna with Metallic strips load

This section presents a circularly polarized rectangular dielectric resonator antenna (CP rectangular DRA) loaded with metallic strips. The dielectric resonator (DR) with metallic strips on the top surface is excited by a simple rectangular aperture feed that excites two degenerative modes to provide circular polarization. The proposed CP rectangular DRA does not require any special dielectric resonator and simplifies the overall design. A prototype of the proposed antenna has been fabricated and validated. It has measured impedance bandwidth between 4.8 and 5.6 GHz and 3dB axial ratio (AR) bandwidth between 5.1 and 5.43 GHz. The axial ratio beamwidth is more than 155^0 in the XZ and YZ planes are obtained.

4.3.1 Proposed Antenna Design and Analysis

The antenna design producer can be summarized as follows. (1) Design a rectangular DRA for a single resonant frequency. (2) Metallic strips are placed on the rectangular DRA to produce CP (generate orthogonal modes) by resonating other lower band frequencies. (3) Antenna parameters were optimized for good impedance matching and axial ratio performance.

The schematic diagram of the proposed CP rectangular DRA with metallic strips load is shown in figure 4.18. The Rogers TMM10i is the dielectric resonator of rectangular shape with a x b dimension and height of 6.3 mm with relative permittivity ϵ_r = 9.8. A rectangular slot is fabricated on a 50 X 50 ground plane of thickness t=0.035 mm. The dimension of the slot is l_s=10.8 mm and w_s= 2.5 mm. The substrate is Rogers 3053, has a thickness of h_s=1.52mm and relative permittivity ϵ_s=3.6. The microstrip feedline is etched on the bottom side of the substrate of feed length l_f and width w_f. The metallic strips are also engraved on the top surface of rectangular DRA diagonally at 45^0 to the x-y axis.
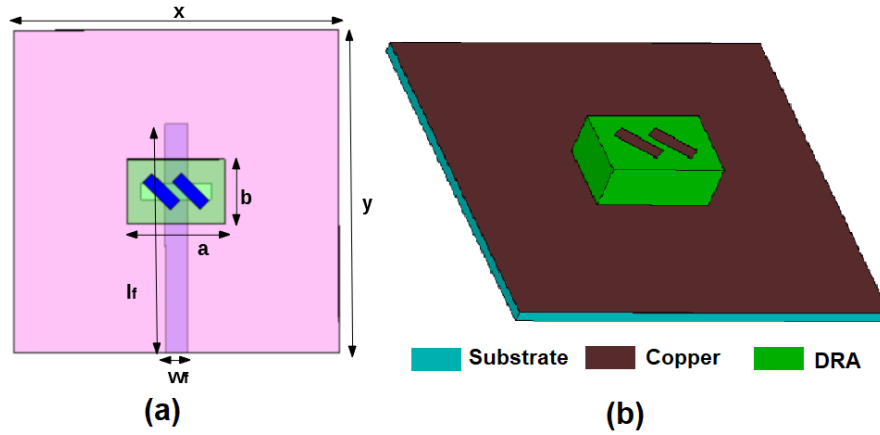
Figure 4.18: (a) Top view of all the layers of the proposed CP RDRA. (b) 3D view of proposed CP RDRA with metallic strips load.(a = 15 mm, b = 10 mm).

Rectangular DRA is designed to resonate at 5.3 GHz with a rectangular slot. It resonates with TE^y111 mode. A good impedance match of 3.7% bandwidth was obtained at 5.3 GHz at l_f = 13 mm, l_s = 10.2 mm, and w_s = 2.5 mm. The circular polarization in (Leung and Ng, 2003) is achieved with a single feed utilizing a parasitic strip/patch. Metal strips act as a load on the DRA, resulting in the excitation of two orthogonal modes with the same amplitude and phase. A pair of metallic strips of length "l" and width "w" is placed on the surface of the rectangular DRA with a separation of 2.6 mm, exciting two orthogonal modes, TE^x_{111} and TE^y_{111} with a phase difference of 90^0.

4.3.2 CP Mechanism

At the interface of dielectric and metal, the charge and surface currents are present (Ellingson, 2018). The tangential component of the magnetic field and the normal component of the electric displacement field are not continuous.

The surface current distribution in the metallic strip on the top of the RDRA at different time instants ($wt = 0^0$ and $wt = 90^0$) is shown in figure 4.19.

The parasitic metallic strips introduce asymmetry in the rectangular DRA, alter the electromagnetic field distribution inside the rectangular DRA and lead to excitation of other resonant modes in the lower frequency band. The metallic strip load changes
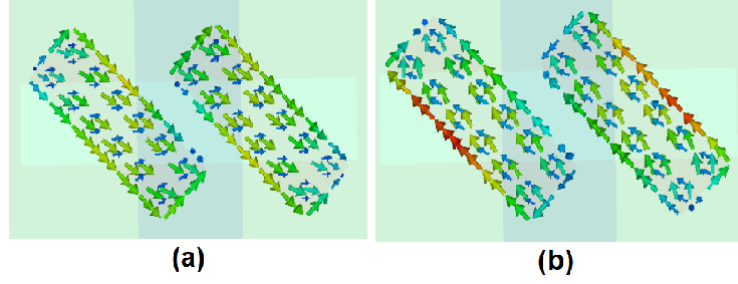
Figure 4.19: Surface current distribution at different time instants (a) wt= 0^0 (b) wt = 90^0.
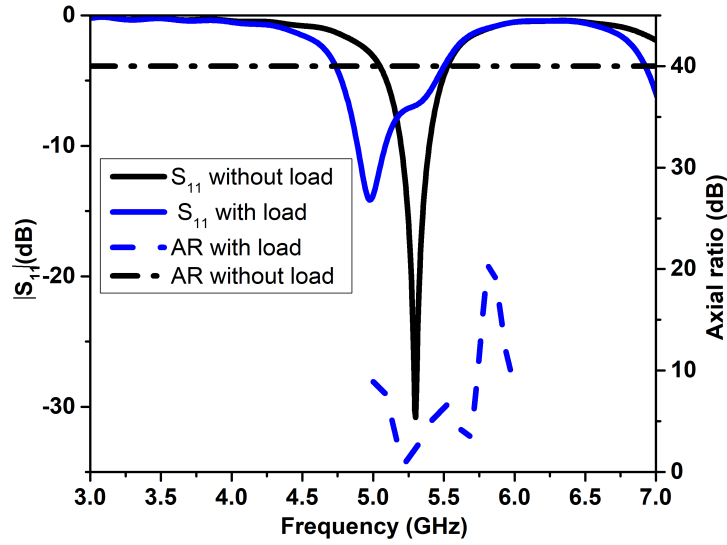
Figure 4.20: Simulated S$_{11}$ and axial ratio of RDRA with and without metallic strips load.

the input impedance characteristic of rectangular DRA, and two resonances were observed. Figure 4.20 shows simulated S_{11} and the axial ratio of rectangular DRA with and without metallic strips load. It is evident from the graph, that the excitation of lower frequency resonance at 4.9 GHz in addition to 5.3 GHz. The axial ratio of less than 3 dB was obtained at 5.25 GHz. The metallic strips placed along the diagonally excite two orthogonal modes, TE^x_{111}, and TE^y_{111}, with a 90^0 phase difference. The frequencies (f_x, f_y) of the two modes are chosen to be equation (4.1) to maximize the AR bandwidth.

$$f_x = \frac{f_o}{1 + \frac{1}{2Q_x}}, f_y = \frac{f_o}{1 - \frac{1}{2Q_y}} \tag{4.1}$$

4.3.3 Parametric study

The parametric study of physical antenna parameters was done to analyze the input impedance and AR bandwidth. A good starting point to obtain circular polarization is selecting the metallic strip length between $\lambda_g/4$ and $\lambda_g/3$. Figure 4.21 and 4.22 show the simulated reflection coefficient and AR for different strip length and width values. The strips parameter affects both the reflection coefficient and axial ratio. The metallic strips length and width helps in improving the S_{11} value once the CP band is obtained. Better impedance value is achieved at l=6 mm and width w=2 mm. Figure 4.23 and 4.24 show the simulated reflection coefficient and AR for different strip length and width values. The feed length provides better impedance match at l_f= 35.5 mm and the axial ratio is not much affected by small variation in feed length. The slot length excites different modes the resonator. The excited modes in the resonator of slot length from 10.2 mm to 11 mm was able provide CP. The two resonances ever clearly distinguishable at slot length of 11 mm.
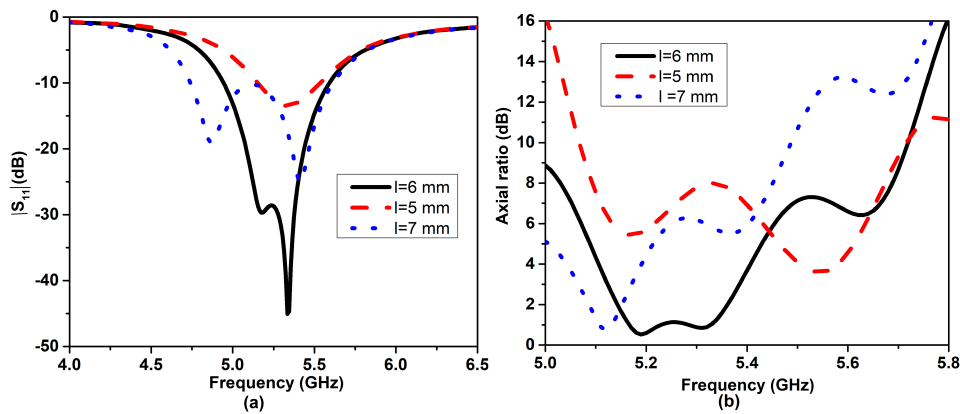
Figure 4.21: Effect of metallic strip length on (a)Reflection coefficient (b)Axial ratio.

4.3.4 Simulation and Measurement results

A prototype of the proposed CP rectangular DRA with metallic strips has been fabricated. The reflection coefficient of the proposed CP rectangular DRA is shown in figure 4.25. The simulated and measured impedance bandwidths are 12.34% and 15.38%
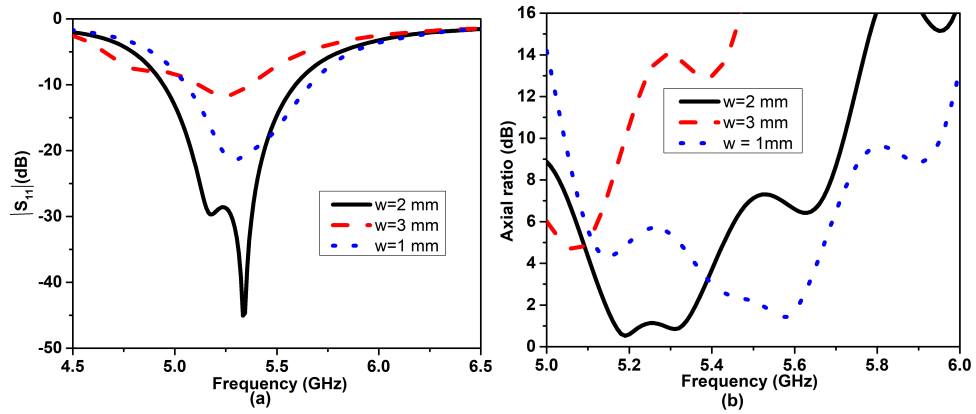
Figure 4.22: Effect of metallic strip width on (a)Reflection coefficient (b)Axial ratio.
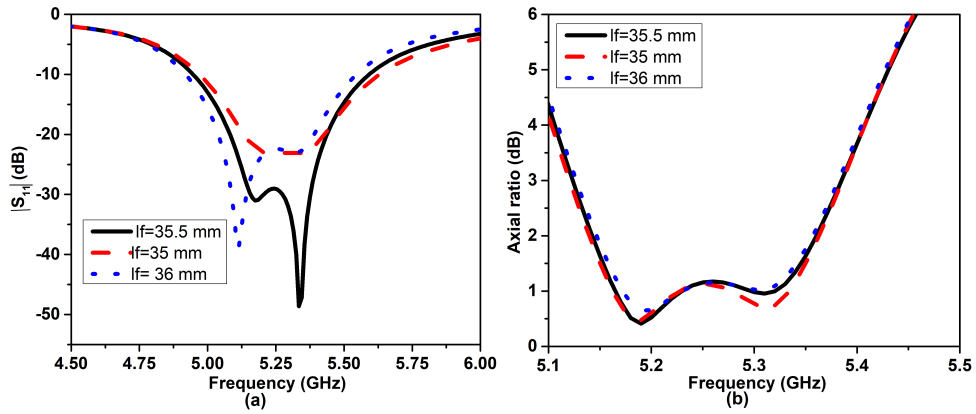
Figure 4.23: Effect of feed length on (a)Reflection coefficient (b)Axial ratio.
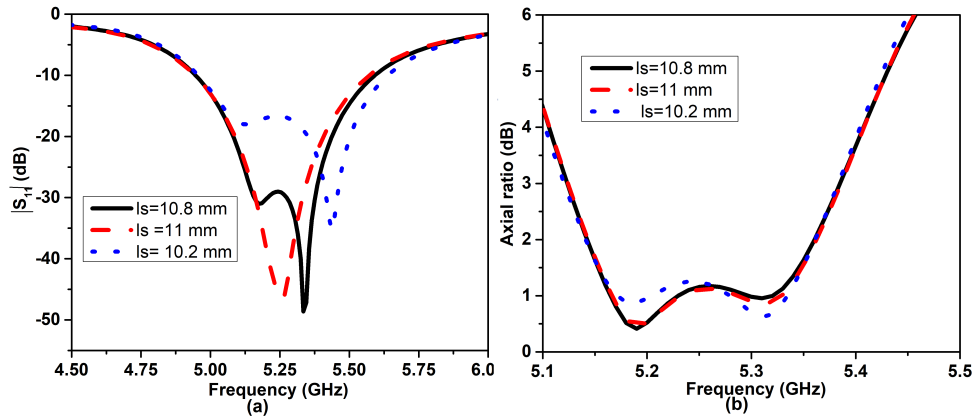
Figure 4.24: Effect of slot length on (a)Reflection coefficient (b)Axial ratio.

($S_{11} \leq$-10dB) within the frequency ranges from 4.94 GHz to 5.59 GHz and from 4.8 GHz to 5.6 GHz, respectively. The axial ratio and gain of the proposed CP rectangular DRA are shown in figure 4.26a. The simulated and measured axial ratio bandwidth

of the CP rectangular DRA are 4.9% and 6.2% ($AR \leq 3$dB) in the boresight direction ($\theta = 0^0$) within the frequency range from 5.12 to 5.38 GHz and from 5.1 to 5.43 GHz, respectively. It can be observed that the axial ratio is around 1 dB for large CP bandwidth. The measured axial ratio bandwidth is approximately 40% of the measured impedance bandwidth. The peak gain of 6.16 dBic is achieved at 5.25 GHz. It is observed that the gain of the proposed antenna remains constant throughout the frequency band with 95% efficiency.

Figure 4.26b shows the variation of axial ratio beamwidth for various azimuth and elevation angles. The simulated axial ratio beamwidth is 158^0 and 167^0 in XY and YZ planes. The measured axial ratio beamwidth is 160^0 and 165^0 in XY and YZ planes respectively.
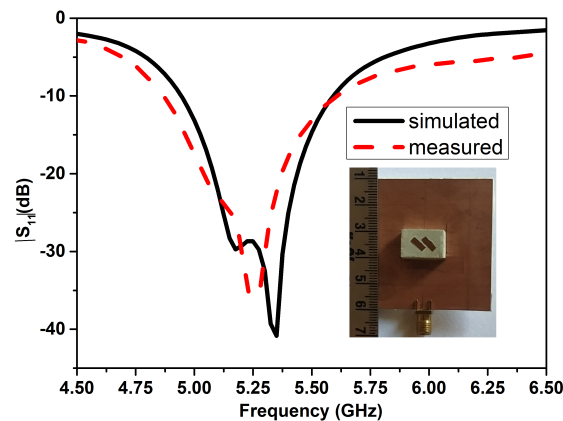
Figure 4.25: Simulated and measured S$_{11}$ of proposed CP RDRA with metallic strips load.

Figure 4.27 shows the antenna's simulated and measured radiation pattern in both azimuth and elevation planes. The antenna radiates the right-hand circular polarization (RHCP) wave in the +z-direction. To prove it, we simulated the electric field distribution in DRA at different time intervals, as shown in figure 4.28. More than a 25 dB difference is achieved between RHCP and left-hand circular polarization (LHCP). The 3 dB radiation beamwidth of 83^0 and 82^0 is obtained in XZ and YZ planes, respectively. The sense of polarization can be reversed by varying the orientation of the metallic strips. Table 4.3 compares existing literature and the CP rectangular DRA with metallic strips load.
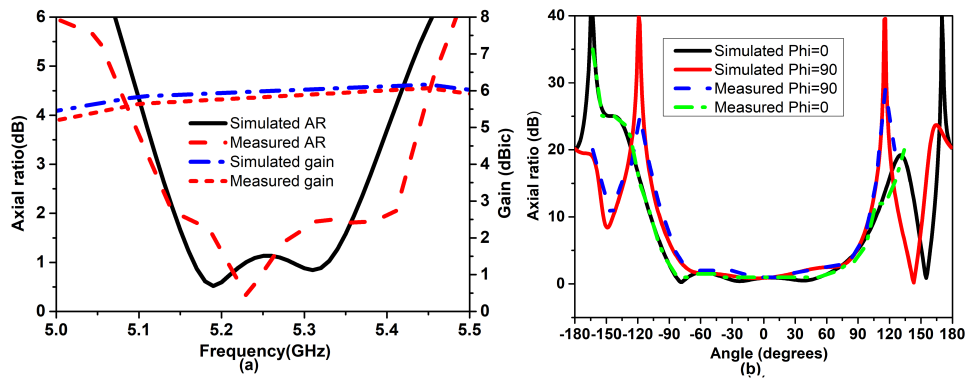
Figure 4.26: (a)Simulated and measured axial ratio and gain of the proposed CP RDRA (b)Simulated and measured axial ratio beamwidth of the proposed CP RDRA.
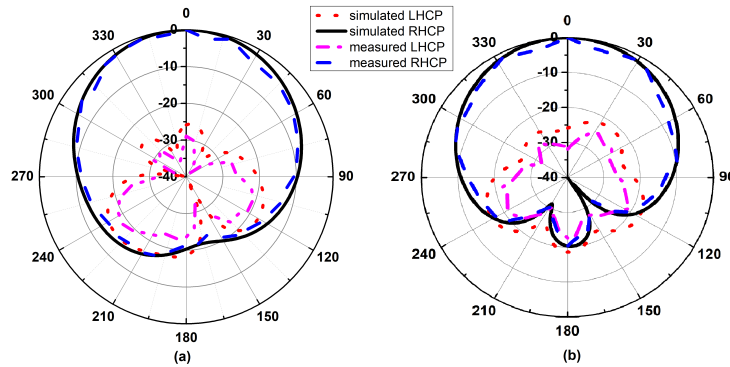
Figure 4.27: Simulated and measured results of normalized radiation patterns of the proposed antenna at 5.25 GHz in the xz and yz planes.
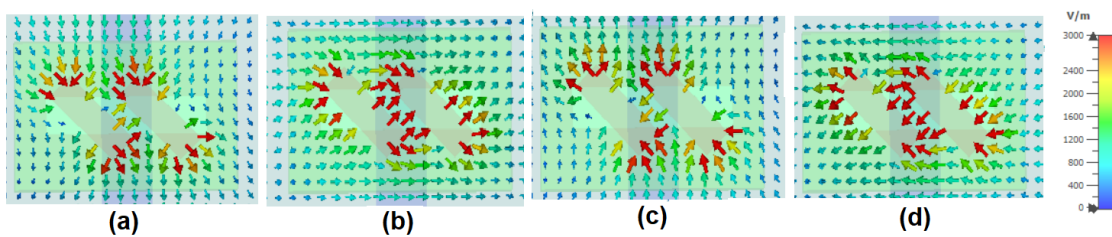
Figure 4.28: Analysis of electric field distribution in the proposed CP RDRA at different instant of time intervals. (a)t=0 (b)t=T/4 (c) t=T/2 (d) t=3T/4.

4.4   Summary

This chapter presents CP antennas using cylindrical and rectangular dielectric resonators. The presented antennas are easy to fabricate with a fundamental dielectric resonator and simple aperture feed. The first section proposes a cylindrical dielectric

Table 4.3: Comparison of present work with earlier reported work.

Feed type	CP technique	DRA Vol (mm^3)	IBW (GHz)	ARBW (GHz)	ARB	Gain (dBi), $\eta(\%)$
Microstrip feed Hsiao et al. (2001)	metallic load	$1.154\lambda_g^3$	2.2-2.3	2.2-2.24	NA	3.3, NA
Coaxial feed Sulaiman and Khamas (2010)	square spiral + metallic strip	$0.748\lambda_g^3$	4-4.44	3.96-4.56	80^0	4, NA
Coaxial feed Sulaiman and Khamas (2011)	metallic strip	$0.336\lambda_g^3$	2.9-3.6	3.1-3.55	115^0, 90^0	5, 98
Aperture coupled Gupta and Gangwar (2018)	slot + patch	$0.311\lambda_g^3$	3.46-3.58 5.1-5.9	3.46-3.54 5.18-5.34	NA	5.4 5.7, 93.7 96.2
Aperture coupled [PW]	slot + metallic load	$0.151\lambda_g^3$	4.8-5.6	5.1-5.43	158^0 167^0	6.16, 95

IBW- Impedance bandwidth, ARBW- Axial ratio bandwidth, ARB-Axial ratio beamwidth, PW-Proposed work

resonator with different hybrid modes. The antenna achieves CP using a flag-shaped feed and a triangular slot. The second section presents a CP antenna that works in the 5GHz ISM band region. The elliptical slot is used for CP generation. A wide axial ration beam width CP rectangular DRA with metallic strips load is presented in the third section. The metallic strips perturb the resonator fields and two nearly degenerate orthogonal modes are generated to achieve CP. The method can be easily applied in array applications. The proposed antenna is suitable for wireless and satellite communication.

CHAPTER 5

Frequency and Pattern Reconfigurable Cylindrical Dielectric Resonator Antenna

Cylindrical dielectric resonator antennas are much used in frequency and pattern reconfiguration due to hybrid excitation modes. However, only a few radiating modes of the cylindrical dielectric resonator are used in antenna designs, such as $TM_{01\delta}$ for omnidirectional pattern, $HEM_{11\delta}$ or $HEM_{12\delta}$ for broadside radiation Mongia and Bhartia (1994). Therefore, exploring the higher-order radiating mode is a hot spot of DRA research.

This work presents a cylindrical dielectric resonator antenna with dual band frequency reconfiguration at 4.8 GHz band and 6.5 GHz. One PIN diode switch is used in the feed line to reconfigure between two bands by turning on and off the switch. A triangular slot is adopted to excite both $HEM_{11\delta}$ and $HEM_{21\delta}$ mode, which provides a broadside and quasi-end-fire beam pattern, respectively.

5.1   Antenna Theory and design

The cylindrical dielectric resonator antenna offers one degree of freedom. It is easy to optimize aspect ratio parameters a/h (a-radius and h-height of the CDRA) to obtain desired radiation characteristics. Hybrid mode radiation is obtained in CDRA. The equations for the fundamental resonant frequency $HEM_{11\delta}$ and higher order mode $HEM_{21\delta}$ are estimated using equation (2.3) and (2.6).

Various feeding methods such as slot aperture, coaxial probe, strips line, etc can be excited in different modes. The location of the feeding point to the DRA establishes the dominant mode Petosa (2007). The $HEM_{11\delta}$ mode is excited when the slot is

placed at the maximum magnetic field intensity in the center of DRA. Aperture feed is easily used to excite $HEM_{11\delta}$ mode Guha et al. (2014). In Gajera et al. (2013) a coaxial cable and metallic perturbation are used to excite $HEM_{21\delta}$ for pattern diversity. The present authors Usha and Krishnamoorthy (2022) used a triangular slot to excite three hybrid modes $HEM_{11\delta}$, $HEM_{21\delta}$ and $HEM_{13\delta}$ in cylindrical DRA. In this paper, frequency reconfiguration is obtained between the two modes $HEM_{11\delta}$ and $HEM_{21\delta}$ using on and off controlling of the PIN diode. Along with frequency reconfiguration, a diversified field pattern is also achieved.

The top and bottom view of the designed cylindrical DRA is shown in figure 5.1. The schematic diagram of the designed cylindrical DRA with a PIN diode is shown in figure 5.2. The dielectric resonator(Rogers TMM10i) has a 10mm radius and height of 6.3mm with relative permittivity ϵ_r = 9.8 is placed on the FR-4 substrate, of thickness hs=0.8mm and relative permittivity ϵ_s=4.3. The triangular slot on a 50mm X 50mm ground plane excites the cylindrical DRA. The microstrip feed line is etched on the bottom side of the substrate of feed width w_1= 1.48mm. One PIN diode in the used feed line is shown the figure 5.1b to achieve reconfigurability.
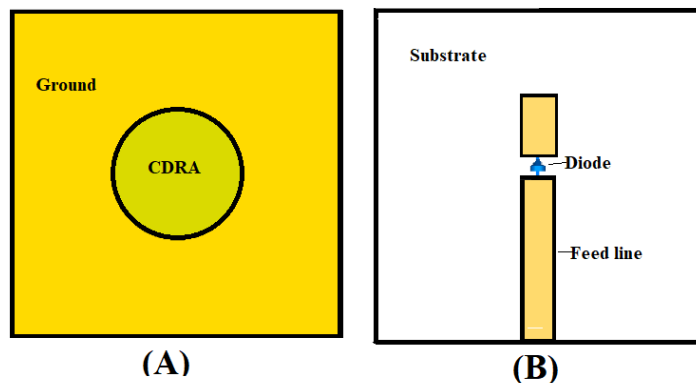
Figure 5.1: (a)Top view and (b)Bottom view of the antenna

5.2 Results and discussions

The simulated results of the antenna are presented. The antenna can operate in two modes depending on the diode is in ON or OFF state. In the figure 5.3, the current
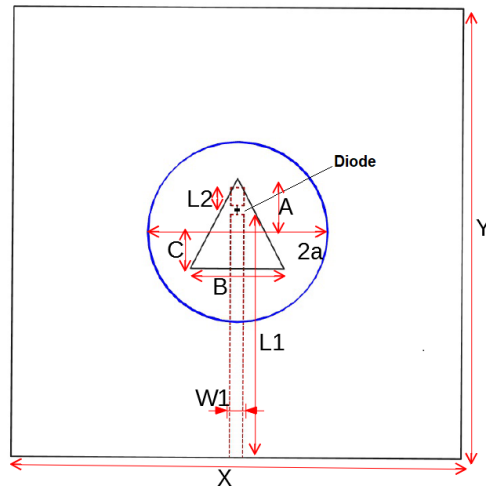
Figure 5.2: Schematic diagram of all the layers of the antenna.(L1=27mm, L2=2mm, A=6mm, C=4mm, B=10.4mm)

distribution observed shows that the ON and OFF conditions of the diode affect the feed length. The change in the feed length varies impedance matching and thereby the resonance frequency changes.
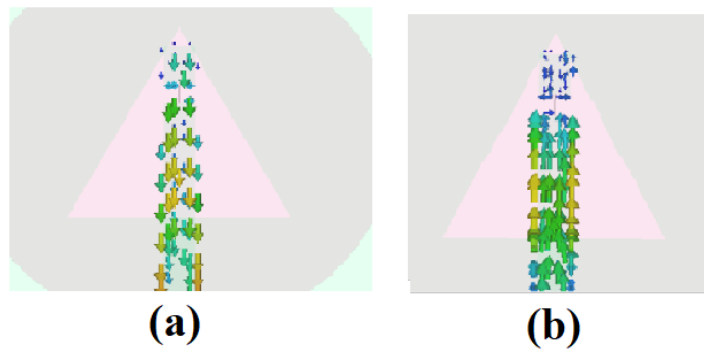
Figure 5.3: Current distribution on feed line at different states of the diode (a)ON state (b)OFF state.

The S_{11} parameter of the antenna is shown in figure 5.4. When the diode is in the ON state, the antenna bandwidth covers the frequency range of 4.64–5.09GHz and when the diode is in the OFF state, the antenna bandwidth is 6.37-6.63GHz.

There is a change in frequency at each state of the switch as a result of a change in the length of the feed. The PIN diode is simulated with lump elements (RLC model). The equivalent circuit of the PIN diode for forward and reverse bias is shown in figure

63
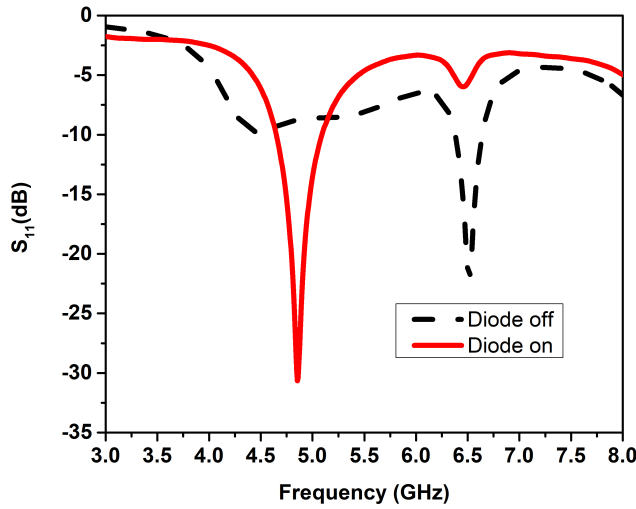
Figure 5.4: Simulated S_{11} of the reconfigurable antenna for different configurations.

5.5.
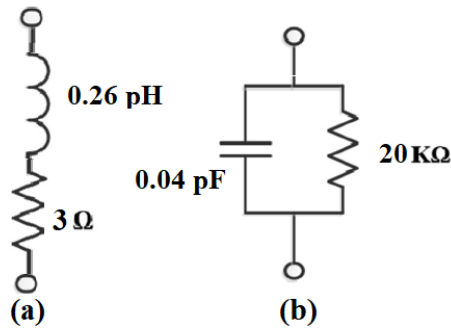
Figure 5.5: Equivalent RLC circuit of PIN diode in (a)ON state (b)OFF state.

To analyze resonant mode, electric field distribution is observed(figure 5.6) and identified as $HEM_{11\delta}$ at 4.8GHz in ON state and $HEM_{21\delta}$ at 6.5GHz in OFF state.

The proposed antenna characteristics are studied in terms of radiation patterns and maximum gain. The radiation pattern curves in the xz-plane and the yz-plane are shown in figures 5.7(a) and 5.7(b) at 4.8GHz and 6.5GHz, respectively. Figure 5.8 illustrates the maximum gain as a function of frequency. The maximum gain at 4.8GHz is 5.5dBi
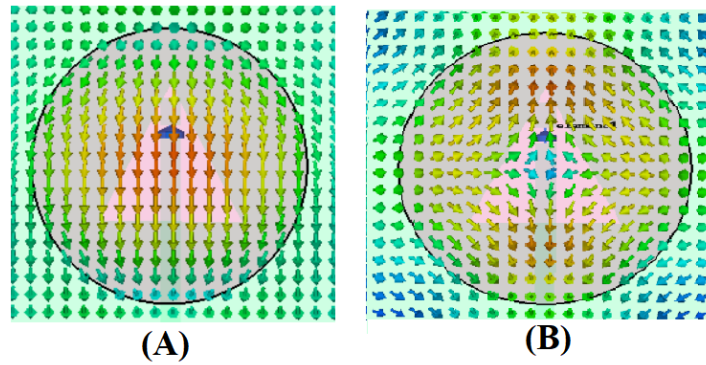
Figure 5.6: Analysis of electric field distribution (a)4.8GHz (b)6.5GHz.

in the boresight and the maximum gain at 6.5GHz is 5.85dBi at theta=43^0 obtained.
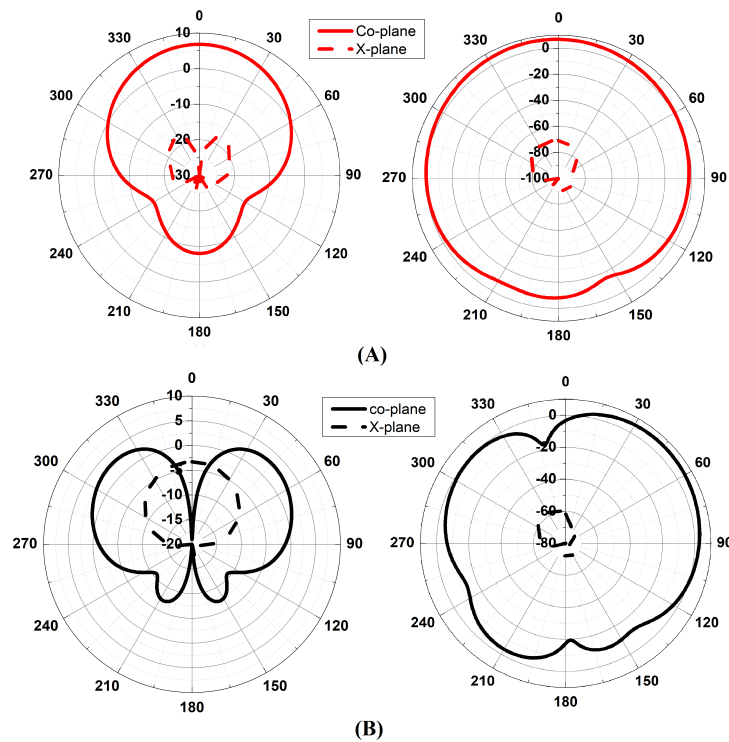
Figure 5.7: Simulated radiation patterns in the xz and yz planes of the antenna at (a)4.8 GHz (b)6.5GHz.
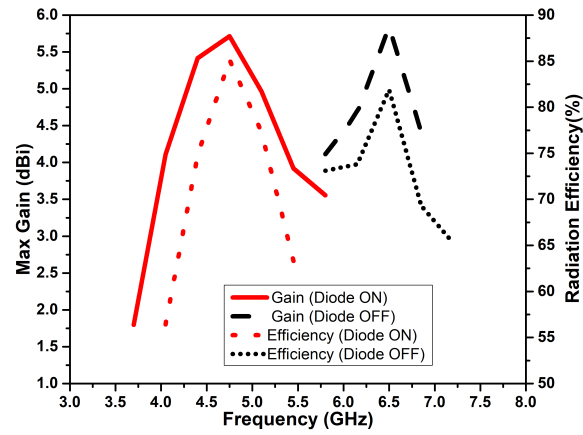
Figure 5.8: Simulated Maximum gain and radiation efficiency of the antenna ON and Off state of the diode.

5.3 Conclusion

The studied a reconfigurable cylindrical DRA with hybrid modes $HEM_{11\delta}$ and $HEM_{21\delta}$ using an aperture feed technique is presented. A reconfigurable cylindrical DRA operates in two different single-band. The pattern diversity is also observed in two bands. The diode was set in the ON state and OFF to obtain the two impedance bands. The designed antenna is suitable for wireless and satellite communication.

CHAPTER 6

CONCLUSION AND FUTURE WORK

Dielectric resonator antennas are preferred because of their advantages over microstrip antennas. Multiband antennas are in demand, where a single antenna can be used for different frequency band applications. Multiband CP antennas are more advantageous in the wireless communication system to overcome multipath interference, environmental effects, fading channels, etc. This research focuses on designing and developing multiband, circularly polarized and frequency reconfigurable antennas. The antennas presented are capable of providing

- Triband and pattern diversity in cylindrical dielectric resonator antenna by exciting higher order hybrid modes.

- Triband Circular polarization and polarization sense in cylindrical dielectric resonator antenna using aperture feeding.

- Circular polarization and polarization sense in rectangular dielectric resonator antenna using aperture feeding and metallic load

- Dual-mode frequency reconfiguration in cylindrical dielectric resonator antenna using PIN diode.

6.1   Contributions

The thesis contribution based on designed antennas is summarized into sections.

6.1.1   Triband cylindrical dielectric resonator antenna

The cylindrical DRA is designed with a fundamental dielectric resonator and aperture coupling with significantly less fabrication complexity. A linear polarized triband cylindrical DRA with a hybrid radiating mode is designed. The higher order modes are excited with simple aperture coupling without suppressing fundamental mode $HEM_{11\delta}$

and weak mode $HEM_{21\delta}$. The antenna also provides pattern diversity. The antenna provides resonances at 4.36, 6.56 and 8.89 GHz with impedance bandwidth of 6.62%, 6.87% and 9.55% and gains of 5.7dBi, 3.9dBi and 8.2dBi, respectively.

6.1.2 Circularly polarized dielectric resonator antennas

In the first design, CP is achieved by overlapping the orthogonal modes excited using elliptical aperture coupling. The elliptical aperture coupled circularly polarized rectangular dielectric resonator antenna provides an axial ratio of 5.88% bandwidth of gain more than 6dBi with a better broadside far-field radiation pattern. The designed antenna completely works in the 5GHz ISM(5.725GHz-5.875GHz) band region. The sense of polarization can be varied by changing the orientation of the elliptical ring slot. The proposed antenna has a conventional rectangular dielectric with a simple excitation technique and easy fabrication that can be used in modern wireless CP applications. In the second design, CP is achieved by degenerative modes. The triband CP characteristic is obtained using the triangular slot and flag-shaped feed line in cylindrical DRA. The antenna provides three impedance bandwidths of 13.02%, 17.9% and 19.51%, and three CP bands 1.39%, 1.21% and 0.31% in the third impedance band. Two RHCP and one LHCP band are obtained. The sense of polarization can be varied by changing the orientation of the flag-shaped feed. CP is also achieved by overlapping the orthogonal modes generated by the slot and field perturbation technique. A low profile wide axial ratio beamwidth CP rectangular DRA with metallic strips load is presented. The metallic strips perturb the rectangular DRA fields, resulting in two orthogonal modes that produce circular polarization. The method can easily be applied to a conventional DRA with a single feed. The proposed antenna is suitable for applications like wireless and satellite communication. The proposed prototypes are fabricated and verified experimentally.

6.1.3 Reconfigurable cylindrical dielectric resonator antenna

A reconfigurable CDRA was presented to support two single-band operations. In this design, we studied a reconfigurable DR with hybrid modes $HEM_{11\delta}$ and $HEM_{21\delta}$ using an aperture feed technique. The pattern diversity is also observed in two bands. The diode was set in the ON and OFF state to obtain the two impedance bandwidth. The proposed antenna is suitable for wireless and satellite communication.

6.2 Future Work

In the present era, wireless communication needs multiband, circularly polarized and frequency reconfigurable dielectric resonator antennas. The presented designs can be further extended to achieve multiband circular polarization antennas. The CP DRAs can be easily applied to array antennas to increase gain in satellite communication. Polarization and pattern reconfigurable antennas are more suitable for MIMO applications. Liquid DRA are evolving due to their low cost, high radiation efficiency and miniaturization. Research on wireless Implantable Medical Devices (IMDs) and other implantable sensors has increased over the last decade using DRAs. Miniaturization is possible in DRA if high permittivity dielectric materials are chosen, which can easily be used in implant antenna. DRA technology offers a cost-effective and high-performance solution for 5G wireless communications. The antenna design can be further extended to millimeter wave, nanophotonics applications and textile-based DRA for wearable Antenna.

LIST OF PUBLICATIONS BASED ON THESIS

Peer reviewed International Journals

- L,Usha and Kanadaamy, Krishnamoorthy. Circularly polarized rectangular dielectric resonator antenna with elliptical aperture feed for 5GHz ISM band. International Journal of RF and Microwave Computer-Aided Engineering. DOI: 10.1002/mmce.22882. Aug 2021.

- Usha L and Krishnamoorthy K, "Linearly Polarized and Circularly Polarized Cylindrical Dielectric Resonator Antenna," Progress In Electromagnetics Research Letters, Vol. 102, 57-65, Jan 2022.

- L,Usha and Kanadaamy, Krishnamoorthy,"Circularly Polarized Rectangular Dielectric Resonator Antenna with Metallic strips load". Microwave and Optical Technology Letters, DOI: doi.org/10.1002/mop.33288. April 2022

International Conferences

- L,Usha and Kanadaamy, Krishnamoorthy. Frequency and pattern Reconfigurable Cylindrical Dielectric Resonator Antenna. IEEE Microwave and Antenna Propoagation (MAPCON) 2022, Bangalore

CURRICULUM VITAE

Name	USHA L
Address	Jaigurudev,
	Manjunath Nagar Bus Stop,
	Kyathasandra,Tumkur -572104
	Karnataka, India
E-mail	lusharamesh@gmail.com
Qualification	• M.Tech | Digital Electronics | VTU University Karnataka
	• B.E | Electronics and Communication Engineering | VTU University Karnataka
Experience	• Assistant Professor | Siddaganga Institute of Technology, Tumakuru.
Experience	• Assistant Lecturer | Sri Siddhartha Institute of Technology, Tumakuru.

REFERENCES

Akhtar, Muhammad Waseem, Syed Ali Hassan, Rizwan Ghaffar, Haejoon Jung, Sahil Garg, and M Shamim Hossain (2020), "The shift to 6g communications: vision and requirements." *Human-centric Computing and Information Sciences*, 10, 1–27.

Apperley, Thomas and Michal Okoniewski (2014), "An air-gap-based frequency switching method for the dielectric resonator antenna." *IEEE Antennas and Wireless Propagation Letters*, 13, 455–458.

Balanis, Constantine A (2005), *Antenna theory: analysis and design*. Wiley-Interscience.

Bemani, M, S Nikmehr, and H Younesiraad (2011), "A novel small triple band rectangular dielectric resonator antenna for wlan and wimax applications." *Journal of Electromagnetic Waves and Applications*, 25, 1688–1698.

Chen, Hua-Ming, Yang-Kai Wang, Yi-Fang Lin, Shih-Chieh Lin, and Shan-Cheng Pan (2008), "A compact dual-band dielectric resonator antenna using a parasitic slot." *IEEE Antennas and Wireless Propagation Letters*, 8, 173–176.

Danesh, S, SKA Rahim, M Abedian, and MR Hamid (2014), "A compact frequency-reconfigurable dielectric resonator antenna for lte/wwan and wlan applications." *IEEE antennas and wireless propagation letters*, 14, 486–489.

Danesh, Sh, SKA Rahim, M Abedian, M Khalily, and MR Hamid (2013), "Frequency-reconfigurable rectangular dielectric resonator antenna." *IEEE antennas and wireless propagation letters*, 12, 1331–1334.

Desjardins, J, DA McNamara, S Thirakoune, and A Petosa (2012), "Electronically frequency-reconfigurable rectangular dielectric resonator antennas." *IEEE transactions on antennas and propagation*, 60, 2997–3002.

Ding, Yong and Kwok Wa Leung (2009), "On the dual-band dra-slot hybrid antenna." *IEEE Transactions on Antennas and Propagation*, 57, 624–630.

Ellingson, Steven (2018), *Electromagnetics Volume 1 (beta)*. Virginia Tech Libraries.

Fakhte, Saeed, Homayoon Oraizi, Reza Karimian, and Rasoul Fakhte (2015), "A new wideband circularly polarized stair-shaped dielectric resonator antenna." *IEEE Transactions on Antennas and Propagation*, 63, 1828–1832.

Fang, Xiao Sheng and Kwok Wa Leung (2012), "Linear-/circular-polarization designs of dual-/wide-band cylindrical dielectric resonator antennas." *IEEE Transactions on Antennas and Propagation*, 60, 2662–2671.

Fang, Xiaosheng, Kwok Wa Leung, and Eng Hock Lim (2014), "Singly-fed dual-band circularly polarized dielectric resonator antenna." *IEEE antennas and wireless propagation letters*, 13, 995–998.

Gajera, Halappa R, Chandrakanta Kumar, Poulomi Gupta, and Debatosh Guha (2013), "Single coax-fed cylindrical dielectric resonator antenna using higher order mode for pattern diversity." *2013 IEEE Applied Electromagnetics Conference (AEMC)*, 1–2, IEEE.

Garg, Ramesh, Prakash Bhartia, Inder J Bahl, and Apisak Ittipiboon (2001), *Microstrip antenna design handbook*. Artech house.

Guha, D., P. Gupta, and C. Kumar (2015), "Dualband cylindrical dielectric resonator antenna employing $\mathrm{hem}_{11\delta}$ and $\mathrm{hem}_{12\delta}$ modes excited by new composite aperture." *IEEE Transactions on Antennas and Propagation*, 63, 433–438.

Guha, Debatosh, Archita Banerjee, Chandrakanta Kumar, and Yahia MM Antar (2011), "Higher order mode excitation for high-gain broadside radiation from cylindrical dielectric resonator antennas." *IEEE Transactions on Antennas and Propagation*, 60, 71–77.

Guha, Debatosh, Poulomi Gupta, and Chandrakanta Kumar (2014), "Dualband cylindrical dielectric resonator antenna employing $hem_{11\delta}$ and $hem_{12\delta}$ modes excited by new composite aperture." *IEEE Transactions on Antennas and Propagation*, 63, 433–438.

Guha, Debatosh and Chandrakanta Kumar (2016), "Microstrip patch versus dielectric resonator antenna bearing all commonly used feeds: An experimental study to choose the right element." *IEEE Antennas and Propagation Magazine*, 58, 45–55.

Gupta, Anshul and Ravi Kumar Gangwar (2018), "Dual-band circularly polarized aperture coupled rectangular dielectric resonator antenna for wireless applications." *IEEE Access*, 6, 11388–11396.

Gupta, Poulomi, Debatosh Guha, and Chandrakanta Kumar (2021), "Dual-mode cylindrical dra: Simplified design with improved radiation and bandwidth." *IEEE Antennas and Wireless Propagation Letters*.

Hsiao, Fu-Ren, Tzung-Wern Chiou, and Kin-Lu Wong (2001), "Circularly polarized low-profile square dielectric resonator antenna with a loading patch." *Microwave and Optical Technology Letters*, 31, 157–159.

Huitema, Laure and Thierry Monédière (2012), "Dielectric materials for compact dielectric resonator antenna applications." *Dielectric Material*, 27.

Jung, Hooin and Chulhun Seo (2002), "Analysis of elliptical microstrip patch antenna considering attachment mode." *IEEE Transactions on Antennas and Propagation*, 50, 888–890.

Kajfez, Darko, Allen W Glisson, and Joseph James (1984), "Computed modal field distributions for isolated dielectric resonators." *IEEE transactions on Microwave Theory and Techniques*, 32, 1609–1616.

Khan, Rizwan, Mohd H Jamaluddin, Jalil Ur Rehman Kazim, Jamal Nasir, and Owais Owais (2016), "Multiband-dielectric resonator antenna for lte application." *IET Microwaves, Antennas & Propagation*, 10, 595–598.

Kishk, AA, KF Lee, D Kajfez, et al. (2006), "Performance comparisons between dielectric resonator antennas and printed microstrip patch antennas at x-band." *Microwave Journal*, 49.

Kumar, Rajkishor and Raghvendra Kumar Chaudhary (2018a), "Circularly polarized rectangular dra coupled through orthogonal slot excited with microstrip circular ring feeding structure for w i-max applications." *International Journal of RF and Microwave Computer-Aided Engineering*, 28, e21153.

Kumar, Rajkishor and Raghvendra Kumar Chaudhary (2018b), "Investigation of higher order modes excitation through f-shaped slot in rectangular dielectric resonator antenna for wideband circular polarization with broadside radiation characteristics." *International Journal of RF and Microwave Computer-Aided Engineering*, 28, e21281.

Kumar, Rajkishor, Sreenath Reddy Thummaluru, and Raghvendra Kumar Chaudhary (2019), "Improvements in wi-max reception: A new dual-mode wideband circularly polarized dielectric resonator antenna." *IEEE Antennas and Propagation Magazine*, 61, 41–49.

Kumari, Reena and Ravi Kumar Gangwar (2018), "Circularly polarized rectangular dielectric resonator antenna fed by a cross aperture coupled spiral microstrip line." *International Journal of RF and Microwave Computer-Aided Engineering*, 28, e21200.

Lee, MT, KM Luk, KW Leung, and MK Leung (2002), "A small dielectric resonator antenna." *IEEE Transactions on Antennas and Propagation*, 50, 1485–1487.

Leung, KM and KW Luk (2003), "Dielectric resonator antenna." *Baldock, Inglaterra: Research Studies Press, Ltd*.

Leung, KW, WC Wong, KM Luk, and EKN Yung (2000), "Circular-polarised dielectric resonator antenna excited by dual conformal strips." *Electronics Letters*, 36, 484–486.

Leung, Kwok Wa and Hoi Kuen Ng (2003), "Theory and experiment of circularly polarized dielectric resonator antenna with a parasitic patch." *IEEE Transactions on Antennas and Propagation*, 51, 405–412.

Lin, Irene Kong Cheh, Mohd Haizal Jamaluddin, Azlan Awang, Raghuraman Selvaraju, Muhammad Hashim Dahri, Leow Chee Yen, and Hasliza A Rahim (2019), "A triple band hybrid mimo rectangular dielectric resonator antenna for lte applications." *IEEE Access*, 7, 122900–122913.

Long, S, Mark McAllister, and Liang Shen (1983), "The resonant cylindrical dielectric cavity antenna." *IEEE Transactions on Antennas and Propagation*, 31, 406–412.

Mongia, Rajesh K and Prakash Bhartia (1994), "Dielectric resonator antennas—a review and general design relations for resonant frequency and bandwidth." *International Journal of Microwave and Millimeter-Wave Computer-Aided Engineering*, 4, 230–247.

Motevasselian, A., A. Ellgardt, and B. L. G. Jonsson (2013), "A circularly polarized cylindrical dielectric resonator antenna using a helical exciter." *IEEE Transactions on Antennas and Propagation*, 61, 1439–1443.

Mun, Byeonggwi, Changwon Jung, Myun-Joo Park, and Byungje Lee (2014), "A compact frequency-reconfigurable multiband lte mimo antenna for laptop applications." *IEEE Antennas and Wireless Propagation Letters*, 13, 1389–1392.

Pan, Yong Mei, Shao Yong Zheng, and Weiwei Li (2014), "Dual-band and dual-sense omnidirectional circularly polarized antenna." *IEEE Antennas and Wireless Propagation Letters*, 13, 706–709.

Patel, Pragati, Biswajeet Mukherjee, and Jayanta Mukherjee (2015), "Wideband circularly polarized rectangular dielectric resonator antennas using square-shaped slots." *IEEE Antennas and Wireless Propagation Letters*, 15, 1309–1312.

Pendharker, Sarang, RK Shevgaonkar, and AN Chandorkar (2014), "Optically controlled frequency-reconfigurable microstrip antenna with low photoconductivity." *IEEE antennas and wireless propagation letters*, 13, 99–102.

Petosa, Aldo (2007), *Dielectric resonator antenna handbook*. Artech House Publishers.

78

Petosa, Aldo and Apisak Ittipiboon (2010), "Dielectric resonator antennas: A historical review and the current state of the art." *IEEE antennas and Propagation Magazine*, 52, 91–116.

Pozar, David M (2011), *Microwave engineering*. John wiley & sons.

Richtmyer, RD (1939), "Dielectric resonators." *Journal of Applied Physics*, 10, 391–398.

San Ngan, Hon, Xiao Sheng Fang, and Kwok Wa Leung (2012), "Design of dual-band circularly polarized dielectric resonator antenna using a higher-order mode." *2012 IEEE-APS Topical Conference on Antennas and Propagation in Wireless Communications (APWC)*, 424–427, IEEE.

Sharma, A, P Ranjan, and RK Gangwar (2017a), "Multiband cylindrical dielectric resonator antenna for wlan/wimax application." *Electronics Letters*, 53, 132–134.

Sharma, Anand, Gourab Das, and Ravi Kumar Gangwar (2017b), "Dual-band dual-polarized hybrid aperture-cylindrical dielectric resonator antenna for wireless applications." *International Journal of RF and Microwave Computer-Aided Engineering*, 27, e21092.

Sharma, Anand, Gourab Das, Surbhi Gupta, and Ravi Kumar Gangwar (2020), "Quad-band quad-sense circularly polarized dielectric resonator antenna for gps/cnss/wlan/wimax applications." *IEEE Antennas and Wireless Propagation Letters*, 19, 403–407.

Sharma, Satish K and Manveer K Brar (2013), "Aperture-coupled pentagon shape dielectric resonator antennas providing wideband and multiband performance." *Microwave and Optical Technology Letters*, 55, 395–400.

Sulaiman, Mohamad I and Salam K Khamas (2010), "A singly fed rectangular dielectric resonator antenna with a wideband circular polarization." *Ieee antennas and wireless propagation letters*, 9, 615–618.

Sulaiman, Mohamad I and Salam K Khamas (2011), "A singly fed wideband circularly polarized dielectric resonator antenna using concentric open half-loops." *IEEE Antennas and Wireless Propagation Letters*, 10, 1305–1308.

Sun, Wen-Jian, Wen-Wen Yang, Peng Chu, and Jian-Xin Chen (2018), "Design of a wideband circularly polarized stacked dielectric resonator antenna." *IEEE Transactions on Antennas and Propagation*, 67, 591–595.

Usha, Lakshminarayana and Kandasamy Krishnamoorthy (2022), "Linearly polarized and circularly polarized cylindrical dielectric resonator antenna." *Progress In Electromagnetics Research Letters*, 102, 57–65.

Varshney, Gaurav, Shailza Gotra, VS Pandey, and RS Yaduvanshi (2018), "Inverted-sigmoid shaped multiband dielectric resonator antenna with dual-band circular polarization." *IEEE Transactions on Antennas and Propagation*, 66, 2067–2072.

Varshney, Gaurav, VS Pandey, RS Yaduvanshi, and Lalit Kumar (2016), "Wide band circularly polarized dielectric resonator antenna with stair-shaped slot excitation." *IEEE Transactions on Antennas and Propagation*, 65, 1380–1383.

Venanzoni, Giuseppe, Davide Mencarelli, Antonio Morini, Marco Farina, and Francesco Prudenzano (2019), "Review of substrate integrated waveguide circuits for beam-forming networks working in x-band." *Applied Sciences*, 9, 1003.

Wang, Daoyu, Min Wang, Nuo Xu, and Wen Wu (2017), "Improved measurement method of circularly-polarized antennas based on linear-component amplitudes." *Open Journal of Antennas and Propagation*, 5, 36–45.

Wang, Kai Xu and Hang Wong (2014), "A circularly polarized antenna by using rotated-stair dielectric resonator." *IEEE Antennas and Wireless Propagation Letters*, 14, 787–790.

Wu, Ke, Dominic Deslandes, and Yves Cassivi (2003), "The substrate integrated circuits-a new concept for high-frequency electronics and optoelectronics." *6th International Conference on Telecommunications in Modern Satellite, Cable and Broadcasting Service, 2003. TELSIKS 2003.*, 1, P–III, IEEE.

Yan, Jie-Bang and Jennifer T Bernhard (2011), "Design of a mimo dielectric resonator antenna for lte femtocell base stations." *IEEE Transactions on Antennas and Propagation*, 60, 438–444.

Yang, Nan and Kwok Wa Leung (2019), "Compact cylindrical pattern-diversity dielectric resonator antenna." *IEEE Antennas and Wireless Propagation Letters*.

Zainud-Deen, Saber H, Mona M Badawy, and Hend A Malhat (2019), "Dielectric resonator antenna loaded with metamaterial polarizer for circular polarization." *2019 36th National Radio Science Conference (NRSC)*, 76–83, IEEE.

Zhou, Yao-Dong, Yong-Chang Jiao, Zi-Bin Weng, and Tao Ni (2015), "A novel single-fed wide dual-band circularly polarized dielectric resonator antenna." *IEEE Antennas and Wireless Propagation Letters*, 15, 930–933.

Zou, Longfang and Christophe Fumeaux (2011), "A cross-shaped dielectric resonator antenna for multifunction and polarization diversity applications." *IEEE Antennas and Wireless Propagation Letters*, 10, 742–745.

Zou, Meng and Jin Pan (2014), "Wideband hybrid circularly polarised rectangular dielectric resonator antenna excited by modified cross-slot." *Electronics Letters*, 50, 1123–1125.

Zou, Meng and Jin Pan (2015), "Wide dual-band circularly polarized stacked rectangular dielectric resonator antenna." *IEEE Antennas and Wireless Propagation Letters*, 15, 1140–1143.

Zou, Meng, Jin Pan, and Zaiping Nie (2015), "A wideband circularly polarized rectangular dielectric resonator antenna excited by an archimedean spiral slot." *IEEE Antennas and Wireless Propagation Letters*, 14, 446–449.

Zou, Meng, Jin Pan, Zaiping Nie, and Pengcheng Li (2013), "A wideband circularly polarized rectangular dielectric resonator antenna excited by a lumped resistively loaded monofilar-spiral-slot." *IEEE Antennas and Wireless Propagation Letters*, 12, 1646–1649.